HHS Public Access

Author manuscript

Cell Rep. Author manuscript; available in PMC 2020 July 27.

Published in final edited form as:

Cell Rep. 2020 June 30; 31(13): 107818. doi:10.1016/j.celrep.2020.107818.

Adipocyte-Derived Versican and Macrophage-Derived Biglycan Control Adipose Tissue Inflammation in Obesity

Chang Yeop Han[1], **Inkyung Kang**[3], **Ingrid A. Harten**[3], **John A. Gebe**[3], **Christina K. Chan**[3], **Mohamed Omer**[1], **Kimberly M. Alonge**[1], **Laura J. den Hartigh**[1], **Diego Gomes Kjerulf**[1], **Leela Goodspeed**[1], **Savitha Subramanian**[1], **Shari Wang**[1], **Francis Kim**[2], **David E. Birk**[4], **Thomas N. Wight**[3], **Alan Chait**[1,5,*]

[1]Department of Medicine, Division of Metabolism, Endocrinology, and Nutrition, University of Washington, Seattle, WA, USA

[2]Division of Cardiology, University of Washington, Seattle, WA, USA

[3]Matrix Biology Program, Benaroya Research Institute, Seattle, WA, USA

[4]Department of Molecular Pharmacology & Physiology, University of South Florida, Tampa, FL, USA

[5]Lead Contact

SUMMARY

Obesity is characterized by adipose tissue inflammation. Because proteoglycans regulate inflammation, here we investigate their role in adipose tissue inflammation in obesity. We find that adipose tissue versican and biglycan increase in obesity. Versican is produced mainly by adipocytes and biglycan by adipose tissue macrophages. Both proteoglycans are also present in adipose tissue from obese human subjects undergoing gastric bypass surgery. Deletion of adipocyte-specific versican or macrophage-specific biglycan in mice reduces macrophage accumulation and chemokine and cytokine expression, although only adipocyte-specific versican deletion leads to sustained improvement in glucose tolerance. Macrophage-derived biglycan activates inflammatory genes in adipocytes. Versican expression increases in cultured adipocytes exposed to excess glucose, and adipocyte-conditioned medium stimulates inflammation in resident peritoneal macrophages, in part because of a versican breakdown product, versikine. These findings provide insights into the role of adipocyte- and macrophage-derived proteoglycans in adipose tissue inflammation in obesity.

Graphical Abstract

*Correspondence: achait@uw.edu.

AUTHOR CONTRIBUTIONS

C.Y.H., I.K., I.A.H., J.A.G., C.K.C., M.O., L.J.d.H., D.G.K., L.G., S.S., K.M.A., and S.W. conducted the experiments. D.E.B. and F.K. contributed essential reagents or tools. All authors interpreted the data and assisted with editing the manuscript. C.Y.H., I.K., T.N.W., and A.C. designed the experiments, supervised the work, interpreted the data, and wrote the manuscript.

DECLARATION OF INTERESTS

The authors declare no competing interests.

SUPPLEMENTAL INFORMATION

Supplemental Information can be found online at https://doi.org/10.1016/j. celrep.2020.107818.

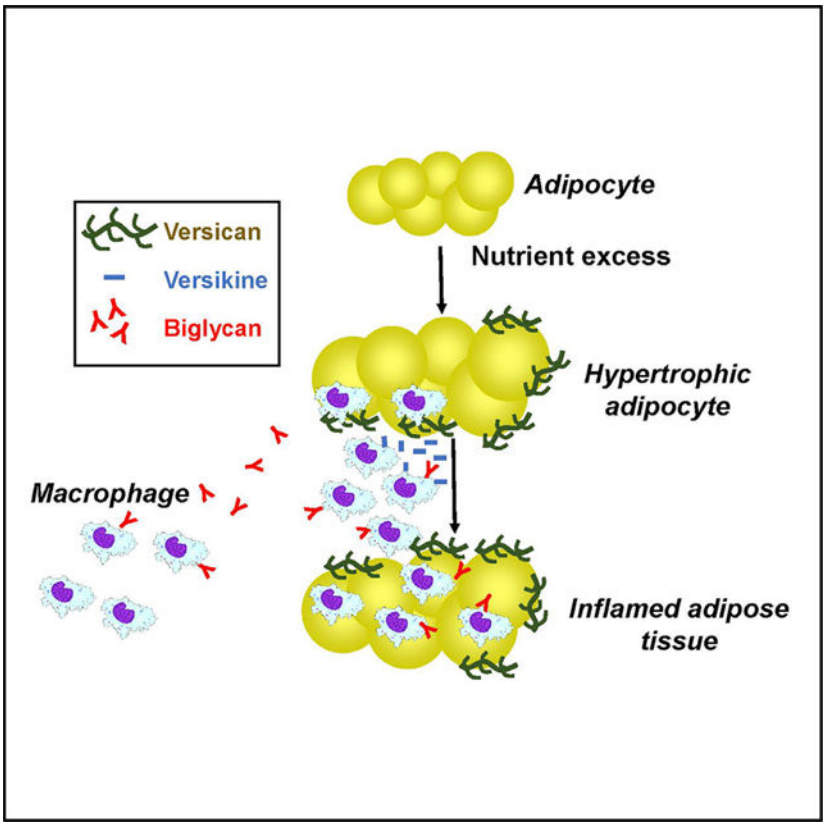

In Brief

Proteoglycans have many functions, including providing a scaffold and regulating the inflammatory response. In this study, Han et al. show that adipose tissue proteoglycans affect inflammation and insulin resistance as a result of crosstalk between versican produced by adipocytes and biglycan produced by macrophages.

INTRODUCTION

Obesity results from a chronic imbalance between energy intake and expenditure. During development of obesity, adipocytes become hypertrophic, and inflammatory cells, such as macrophages, accumulate in adipose tissue (Weisberg et al., 2003; Wellen and Hotamisligil, 2003; Xu et al., 2003). Such changes occur to a greater extent in intra-abdominal (visceral) compared with subcutaneous fat (Cancello et al., 2006; Harman-Boehm et al., 2007). Adipocytes and macrophages in adipose tissue from obese mice and humans produce pro-inflammatory molecules, which are believed to play a role in insulin resistance and systemic inflammation (Bulló et al., 2003; Cancello and Clément, 2006; Maachi et al., 2004).

Extracellular matrix (ECM) molecules and their cleavage products can act as inflammatory modulators (Roedig et al., 2019b; Wight et al., 2014). Adipose tissue makes abundant ECM, which is in a constant state of turnover to accommodate changes in tissue volume associated with fluctuations in energy storage needs (Mariman and Wang, 2010). Several ECM molecules are increased in visceral adipose tissue in genetically obese mice and mice made

obese by consumption of a high-fat diet (Han et al., 2007; Huber et al., 2007; Khan et al., 2009; Spencer et al., 2011). The ECM has also been reported to increase in adipose tissue in human subjects with obesity or diabetes (Divoux et al., 2010; Kim et al., 2016), although the nature and cellular sources of these matrix molecules have yet to be well characterized. To date, most studies of the ECM in adipose tissue have focused on collagen, which has been suggested to form a scaffold that can induce mechanical stress and constrain the expansion of adipocytes during development of obesity (Khan et al., 2009; Spencer et al., 2011; Sun et al., 2014). However, little is known about alterations in other ECM molecules such as proteoglycans, their cellular sources, and their role in adipose tissue inflammation.

We showed previously that hypertrophic adipocytes produce a chondroitin sulfate-rich proteoglycan that can trap high-density lipoproteins (HDLs) isolated from serum of mice and humans with inflammation by binding to serum amyloid A (SAA), which is present on HDL in inflammatory states (Han et al., 2016). We have now identified this proteoglycan as versican, a large chondroitin sulfate-rich proteoglycan found in the ECM of most soft tissues (Wight, 2002). Versican is elevated during development and inflammation (Kang et al., 2018; Snyder et al., 2015; Wight et al., 2020) and regulates events associated with adipose tissue inflammation, such as lipoprotein retention (Williams and Tabas, 1995, 1998), lipid uptake, and foam cell formation (Ismail et al., 1994; Llorente-Cortés et al., 2002; Srinivasan et al., 1995). Versican also influences inflammatory processes by interacting with chemokines, growth factors, proteases, and receptors such as CD44, PSGL-1, and TLR2 on the surface of immune cells to provide intrinsic signals and influence the immune cell phenotype (Hirose et al., 2001; Taylor and Gallo, 2006; Wu et al., 2005).

Another ECM molecule with pro-inflammatory properties found in adipose tissue is biglycan, a small leucine-rich proteoglycan. Although it binds to collagen and can act as a scaffold, it also activates Toll-like receptor 2 (TLR2) and TLR4 (Babelova et al., 2009; Kim et al., 2016; Roedig et al., 2019a; Schaefer et al., 2005). Because biglycan can be made by macrophages, which accumulate in adipose tissue in obesity, we determined whether macrophage-derived biglycan increases in adipose tissue during development of obesity and whether proteoglycans produced in obese adipose tissue influence inflammation.

We now show that versican is produced mainly by adipocytes, whereas biglycan is produced mainly by macrophages, in adipose tissue in mice during development of obesity resulting from consumption of a high-fat, high-sucrose (HFHS) diet. Both proteoglycans have been observed in subcutaneous and omental fat from obese human subjects undergoing gastric bypass surgery. Mice with adipocyte-specific deletion of versican showed a modest improvement in insulin sensitivity with reduced adipose tissue and liver inflammation, whereas mice with macrophage-specific deficiency of biglycan had reduced adipose tissue inflammation. Consistent with these *in vivo* findings, *in vitro* experiments demonstrated that versican expression was increased in hypertrophic 3T3-L1 adipocytes and that biglycan expression was increased in palmitate-stimulated macrophages. Moreover, conditioned medium from palmitate-stimulated resident peritoneal macrophages (RPMs) induced inflammation in adipocytes, which was partially abolished by silencing biglycan expression in the macrophages. Although conditioned medium from hypertrophic adipocytes activated RPMs, the effect was not abolished by silencing versican. However, versikine, a byproduct

of versican proteolytic cleavage by macrophages, increased inflammation in macrophages. In addition, silencing versican in hypertrophic 3T3-L1 adipocytes reduced the ability of monocytes to adhere to the adipocyte-derived ECM. Collectively, these data suggest that crosstalk between adipocytes and macrophages mediated by proteoglycans may play a role in adipose tissue inflammation and insulin sensitivity in obesity.

RESULTS

Versican Is Produced by Adipocytes, and Biglycan Is Produced by Macrophages in Obese Mice

To determine obesity-related ECM changes in adipose tissue in mice, we measured changes in the expression of versican, hyaluronan, and biglycan in epididymal white adipose tissue (EWAT) during progression of obesity resulting from consumption of a HFHS pro-inflammatory obesogenic diet. Versican (*Vcan*), hyaluronan synthase 2 (*Has2*), and biglycan (*Bgn*) gene expression gradually increased between 8 and 16 weeks compared with chow-fed control mice (Figure 1A). The increase in *Has2* confirmed our previous finding that *Has2* expression increased during development of obesity (Han et al., 2007). Immunostaining performed on EWAT after 16 weeks on the diet showed an increase in versican and biglycan immunostaining, whereas perlecan and decorin staining was not changed (Figure 1B). Consistent with these immunostaining data, *Vcan* and *Bgn* gene expression was increased in whole EWAT after 16 weeks (Figure 1C). To investigate which cell types were responsible for these changes, adipocyte-enriched (AE) and macrophage-enriched fractions were isolated. The macrophage markers *F4/80* and *Cd11b*, measured by RT-PCR and western blotting in the AE fractions, were minimally expressed, whereas adiponectin (*Adipoq*) was highly expressed (data not shown), indicating a paucity of macrophages in the AE fractions. *Vcan* and *Has2* gene expression was increased in the AE fraction and *Bgn* gene expression in the macrophage-enriched fraction (Figures 1D and 1E). Expression of chemokines (*Saa3* and *Ccl2*) and cytokines (*Il1b*, *Il6*, and *Tnfa*) increased in AE and macrophage-enriched fractions (Figures 1D and 1E), but the higher copy number for the macrophage-enriched fraction indicates that macrophages were the major source of these molecules (Figure 1E). In a cell fraction negatively selected with a CD11b antibody that included endothelial and vascular cells, pre-adipocytes, and stem cells, expression of these genes was not changed (data not shown). These data suggest that, among these ECM molecules, versican and hyaluronan are produced predominantly by adipocytes and biglycan is produced predominantly by macrophages during development of obesity in mice induced by HFHS feeding.

Versican and Biglycan Are Present in Adipose Tissue from Obese Human Subjects and Are Greater in Omental Than in Subcutaneous Fat

To determine whether similar proteoglycans are present in human obesity, we collected omental and subcutaneous (s.c.) adipose tissue from human subjects undergoing gastric bypass surgery. Among proteoglycans and glycosaminoglycans, *VCAN*, *HAS2*, and *BGN* gene expression was found to be higher in omental than in s.c. adipose tissue, along with increased expression of chemokines (*SAA3* and *CCL2*), cytokines (*IL1B*, *IL6*, and *TNFA*) and the macrophage marker *CD68* (Figure 2A). As shown previously, *ADIPOQ* gene

expression was lower in omental fat (Chen et al., 2012; Kern et al., 2003; Figure 1A). Consistent with our gene expression data, staining for versican, biglycan, and macrophages was increased to a greater extent in omental than in s.c. fat from obese human subjects (Figure 2B). We did not perform similar studies in lean human subjects because of the difficulty in obtaining intra-abdominal adipose tissue from such subjects.

Adipocyte-Specific Deficiency of Versican Results in Improved Insulin Sensitivity and Reduced Adipose Tissue and Liver Inflammation

Because versican was expressed predominantly in adipocytes, to investigate the pathophysiological role of adipocyte-derived versican in diet-induced obesity, we generated adipocyte-specific *Vcan*-deficient (*Adipoq-Cre/+;Vcan*$^{Flox/Flox}$) mice as described in STAR Methods. Adipocyte-specific deletion of versican was verified by genotyping and analysis of *Vcan* gene expression in EWAT, inguinal white adipose tissue (IWAT), brain, heart, smooth muscle, and whole liver. EWAT and IWAT from *Adipoq-Cre/+;Vcan*$^{Flox/Flox}$ mice showed almost complete loss of *Vcan* mRNA, whereas expression was maintained in other tissues (Figure S1B). To assess the effect of adipocyte-specific versican deletion on metabolic homeostasis, we compared weight gain, glucose tolerance, and insulin tolerance in *Adipoq-Cre/+;Vcan*$^{Flox/Flox}$ mice and *Adipoq-Cre/+;Vcan*$^{+/+}$ control mice after 16 weeks on a HFHS diet. No difference between genotypes was observed in body weight during the course of the study (Figure 3A). *Adipoq-Cre/+;Vcan*$^{Flox/Flox}$ mice showed modestly improved glucose and insulin tolerance after 14 and 15 weeks on the diet, respectively. Consistent with this, fasting insulin levels were lower in *Adipoq-Cre/+;Vcan*$^{Flox/Flox}$ mice at 16 weeks. In addition, plasma adiponectin levels were higher in *Adipoq-Cre/+;Vcan*$^{Flox/Flox}$ mice at 16 weeks (Table 1). However, fasting non-esterified fatty acid (NEFA) levels were not changed in *Adipoq-Cre/+;Vcan*$^{Flox/Flox}$ mice and *Adipoq-Cre/+;Vcan*$^{+/+}$ control mice after 16 weeks on a HFHS diet (Table 1).

Because versican could potentially regulate adipocyte differentiation, we determined whether adipogenesis was blunted in *Adipoq-Cre/+;Vcan*$^{Flox/Flox}$ mice. Differentiated adipocytes cultured from stromal vascular cells (SVCs) isolated from EWAT of *Adipoq-Cre/+;Vcan*$^{Flox/Flox}$ and *Adipoq-Cre/+;Vcan*$^{+/+}$ mice showed appropriate levels of lipid droplets (Figure S1C). In addition, expression of adipogenesis genes (*Pparg*, *Adipoq*, *C/ebpa*, *aP2*, and *Glut4*) was not altered in *Adipoq-Cre/+;Vcan-*$^{Flox/Flox}$ mice compared with *Adipoq-Cre/+;Vcan*$^{+/+}$ mice (Figure S1C). Similarly, gene expression of *Pref1*, a marker for pre-adipocytes, was equally diminished in fully differentiated adipocytes from *Adipoq-Cre/+;Vcan*$^{Flox/Flox}$ and *Adipoq-Cre/+;Vcan*$^{+/+}$ mice (Figure S1C). These data suggest that the extent of adipocyte differentiation did not differ between wild-type control and adipocyte-specific versican-deficient mice.

To determine the effect of ablation of adipocyte-derived versican on adipose tissue inflammation in obesity, we investigated the expression of several inflammation genes in adipose tissue after 16 weeks on the HFHS diet. Expression of the macrophage chemotactic factor genes *Saa3* and *Ccl2* and the cytokines *Tnfa* and *Il6* was decreased in EWAT from *Adipoq-Cre/+;Vcan*$^{Flox/Flox}$ mice compared with their littermate controls (*Adipoq-Cre/+;Vcan*$^{+/+}$) (Figure 3B). Similarly, expression of the macrophage markers *Mac2*, *Cd11b*,

Cd11c, and *F4/80* was decreased in EWAT of *Adipoq-Cre/+;Vcan*$^{Flox/Flox}$ mice compared with littermate controls (*Adipoq-Cre/+;Vcan*$^{+/+}$) (Figure 3B). Immunohistochemical staining also showed a decrease in galectin-3 (Mac2) protein in EWAT of *Adipoq-Cre/+;Vcan*$^{Flox/Flox}$ mice compared with controls (Figure 3C). These findings suggest that the absence of versican in adipocytes has an anti-inflammatory effect on EWAT in HFHS diet-induced obesity.

Because adipocyte-specific ablation of versican could affect hepatic physiology via altered adipokine secretion, we also measured the expression of various genes in the livers of adipocyte-specific versican-deficient mice after 16 weeks on the HFHS diet. Expression of the chemokine and pro-inflammatory genes *Saa1*, *Ccl2*, *Il1b*, *Il6*, and *Tnfa* and the macrophage markers *Mac2* and *F4/80* was decreased in the livers of *Adipoq-Cre/+;Vcan*$^{Flox/Flox}$ mice (Figure 3D). However, there were no differences in expression of apolipoprotein A-I (*Apoa1*), peroxisome proliferator-activated receptor gamma coactivator 1α (*Pgc1a*), carnitine palmitoyl transferase 1α (*Cpt1a*), diacylglycerol O-acyltransferase 1 (*Dgat1*), sterol regulatory element-binding protein (*Srebp1*), and *Srebp2* gene expression (Figure 3D). Plasma SAA levels were decreased in *Adipoq-Cre/+;Vcan*$^{Flox/Flox}$ mice at 16 weeks (Table 1). However, *Adipoq-Cre/+;Vcan*$^{Flox/Flox}$ mice showed similar triglyceride and cholesterol levels compared with *Adipoq-Cre/+;Vcan*$^{+/+}$ mice (Table 1). Collectively, these data suggest that adipocyte-specific deletion of versican has beneficial effects on the liver, which could contribute to the observed whole-body insulin sensitization.

Macrophage-Specific Biglycan-Deficient Mice Show Reduced Adipose Tissue but Not Liver Inflammation

Biglycan was predominantly expressed in macrophages in adipose tissue from obese mice. To investigate the pathophysiological role of macrophage-specific biglycan in a diet-induced obesity mouse model, we transplanted CD45.1 isotype recipient *Bgn*$^{+/0}$ mice with bone marrow cells from CD45.2 isotype *Bgn*$^{+/0}$ or whole-body biglycan knockout (*Bgn*$^{-/0}$) donor mice, as described in STAR Methods. We confirmed by fluorescence-activated cell sorting (FACS) analysis that 90% of immune cells in the spleen were reconstituted with CD45.2 isotype cells and that *Bgn* gene expression was drastically reduced in bone marrow-derived macrophages (BMDMs) from *Bgn*$^{-/0}$ transplanted mice compared with *Bgn*$^{+/0}$ transplanted mice (Figure S2). To assess the effect of hematopoietic cell-specific biglycan deletion on metabolic homeostasis, we compared weight gain, glucose tolerance, and insulin tolerance in *Bgn*$^{-/0}$ transplanted and control *Bgn*$^{+/0}$ transplanted mice fed a HFHS diet for 16 weeks. No differences in body weights between chimeric mice were observed during the course of the study (Figure 4A). *Bgn*$^{-/0}$ transplanted mice showed improved glucose tolerance after 8 weeks but not after 16 weeks of HFHS feeding (Figure 4A). There were no differences in insulin tolerance at 8 and 16 weeks on the HFHS diet between these chimeric mice (data not shown). Bone marrow-specific ablation of *Bgn* did not affect fasting insulin levels or plasma cholesterol and triglycerides at 16 weeks on the HFHS diet (Table S1). However, plasma adiponectin levels were higher and fasting NEFA levels were lower in *Bgn*$^{-/0}$ transplanted mice at 16 weeks (Table S1).

Expression of the chemotactic factor genes *Saa3* and *Ccl2* and of the macrophage markers *Mac2*, *Cd11b*, *Cd11c*, and *F4/80* was decreased in EWAT of $Bgn^{-/0}$ transplanted compared with $Bgn^{+/0}$ transplanted controls after 16 weeks on a HFHS diet (Figure 4B). Immunohistochemical staining also showed a decrease in Mac2 protein in EWAT of $Bgn^{-/0}$ transplanted mice (Figure 4C). Interestingly, expression of *Cd206*, a marker for the M2 macrophage phenotype, was increased in EWAT of $Bgn^{-/0}$ transplanted mice compared with $Bgn^{+/0}$ transplanted controls (Figure 4B). To further investigate how M2 macrophages were increased in EWAT of $Bgn^{-/0}$ transplanted mice fed the HFHS diet for 16 weeks, we isolated bone marrow cells from these transplanted mice and differentiated BMDMs into M1 and M2 phenotypes. M2 BMDMs from $Bgn^{-/0}$ transplanted mice showed increased gene expression of the M2 makers arginase 1 (*Arg1*) and *Cd206* compared with M2 BMDMs from $Bgn^{+/0}$ transplanted mice (Figure S3A). Conversely, M1 BMDMs from $Bgn^{-/0}$ transplanted mice showed decreased gene expression of the M1 makers *Nos2* and *Tnfa* compared with BMDMs from $Bgn^{+/0}$ transplanted mice (Figure S3A). These findings suggest that the absence of biglycan in macrophages skews macrophages toward an M2 phenotype, which could promote an anti-inflammatory effect on EWAT during HFHS diet-induced obesity.

To investigate whether this anti-inflammatory effect of biglycan ablation in macrophages also affected liver inflammation, we measured expression of various genes in the livers of macrophage-specific biglycan-deficient mice. Expression of the *Saa1*, *Ccl2*, *Il1b*, *Il6*, and *Tnfa* genes in the livers of $Bgn^{-/0}$ transplanted mice did not differ from those in $Bgn^{+/0}$ transplanted mice after 16 weeks of HFHS feeding (Figure 4D). No differences in expression of *Apoa1*, *Pgc1a*, *Cpt1a*, *Dgat1*, *Srebp1*, and *Srebp2* gene expression were detected between the two groups (Figure 4D). Gene expression of the macrophage markers *Mac2* and *F4/80* also did not differ between the two groups (Figure 4D). Moreover, plasma levels of SAA, a circulating inflammatory marker derived mainly from the liver, were the same in both groups of mice (Table S1). To further investigate why we were unable to observe a reduction in inflammatory gene expression in the liver similar to what we observed in adipose tissue, we took advantage of the fact that we used recipient mice on a CD45.1 and donor mice on a CD45.2 background. Interestingly, unlike what we observed in adipose tissue, in which the pan *Cd45* and *Cd45.2* probes identified the same gene transcript, expression of *Cd45.2* was reduced compared with pan *Cd45* in the liver (Figure S3B). These findings indicate the presence of CD45.1-positive macrophages in the livers of the mice transplanted with biglycan-deficient marrow, suggesting that radio-resistant and long-lived $Bgn^{+/0}$ Kupffer cells still remained in the liver (Klein et al., 2007). These CD45.1-positive cells likely contribute to liver inflammation, whereas macrophages in adipose tissue were rapidly replaced with donor $Bgn^{-/0}$ cells, which resulted in reduced adipose tissue inflammation.

Versican mRNA and Protein Expression Are Increased in Hypertrophic 3T3-L1 Adipocytes *In Vitro*, and Versikine, a Protein Derived from Versican, Stimulates Macrophage Inflammation

To investigate the mechanism by which versican could modulate adipose tissue inflammation, we first determined whether versican is increased when cultured adipocytes become hypertrophic *in vitro*. Fully differentiated 3T3-L1 adipocytes were exposed to high

glucose concentrations to induce hypertrophy, as described previously (Han et al., 2007). After 7 days of growth in 25 mmol/L glucose, 3T3-L1 adipocytes appeared hypertrophic and contained large numbers of lipid droplets compared with cells maintained in 5 mmol/L glucose (Han et al., 2007). Of several ECM genes measured (*Vcan*, *Has2*, *Bgn*, *Prcan*, and *Dcn*), only *Vcan* and *Has2* expression were significantly increased in hypertrophic adipocytes (Figure 5A), as we have shown previously for *Has2* (Han et al., 2007). In confirmation of these gene expression findings, versican—but not biglycan, perlecan, and decorin—was secreted from hypertrophic adipocytes (Figure 5B). In addition, *Vcan* gene expression was increased in other primary mouse adipocytes and human Simpson-Golabi-Behmel syndrome (SGBS) adipocytes incubated with high glucose concentrations (Figure S4). The increase in versican core protein expression after exposure to high glucose concentrations was also associated with changes in the sulfation pattern of the attached chondroitin and dermatan sulfate glycosaminoglycans (CS/DS-GAG), with high glucose conditions producing a significant decrease in the relative expression of Δ4S-and Δ4S6S-CS isomers and a corresponding increase in Δ0S-, Δ6S-, and Δ2S6S-CS isomers and dermatan sulfate (Figure S5). Because we showed previously that monocyte adhesion to hyaluronan in a complex matrix secreted by hypertrophic adipocytes was increased (Han et al., 2007), we next examined whether adipocyte-derived versican could regulate monocyte adhesion to this complex matrix produced by hypertrophic adipocytes. Versican silencing with *Vcan*-specific small interfering RNA (siRNA) reduced monocyte adhesion to hypertrophic adipocytes (Figure 5C), which implies that versican produced by hypertrophic adipocytes could regulate macrophage accumulation in adipose tissue.

To further determine possible pathophysiological roles for adipocyte-derived versican in adipose tissue inflammation, purified versican and versican-containing conditioned medium from hypertrophic 3T3-L1 adipocytes exposed to high glucose was added to RPMs. Although purified versican failed to increase any inflammatory markers in RPMs (Figure 5D), incubation of RPMs with conditioned medium from hypertrophic adipocytes did increase expression of *Saa3*, *Ccl2*, *Tnfa*, *Il1b*, and *Il6* (Figure 5E). The increased expression of these genes was not reduced when quiescent non-activated RPMs were exposed to conditioned medium from adipocytes in which versican was silenced with a *Vcan*-specific siRNA (Figure 5E), suggesting that something other than versican was activating the macrophages.

Activated macrophages can convert versican into a bioactive product, versikine, which signals through TLR2 and increases inflammation in immune cells (Schmitt, 2016). After incubating conditioned medium from hypertrophic adipocytes with RPMs, large versican molecules were partially converted into the smaller versikine (Figure 5F). Addition of purified versikine (Figure S6A) to RPMs increased expression of *Saa3*, *Ccl2*, *Tnfa*, *Il1b*, and *Il6* but not *Bgn* or *Vcan* (Figure 5G). The V0 and V1 core protein of versican, from which versikine is made, also did not increase inflammation in RPMs (Figure S6B). To investigate the mechanism by which versikine affects inflammation and whether versikine regulates insulin signaling in RPMs, we measured phosphorylation of nuclear factor κB (NF-κB) p65 and Akt (Figures S6C and S6D). Versikine activated NF-κB p65 and reduced the sensitivity of insulin signaling in RPMs *in vitro*. These results imply that, although intact versican did not affect inflammation in macrophages, versikine, which can be converted from versican by

proteolytic cleavage by activated macrophages, can increase the expression of some inflammatory genes in macrophages, providing evidence of indirect crosstalk between hypertrophic adipocytes and macrophages in adipose tissue in obesity.

Macrophage-Derived Biglycan Increases Inflammation in Adipocytes

To evaluate the role of macrophage activation as a source of biglycan in obesity, RPMs exposed to palmitate, a known activator of TLR4 (Schaefer et al., 2005), demonstrated increased *Bgn* gene expression along with increased chemokine gene expression (Figure 6A). Tumor necrosis factor alpha (TNF-α) addition to RPMs had a similar effect (Figure 6A). Although *Vcan* gene expression was increased by palmitate and TNF-α, its expression level was very low compared with *Bgn* gene expression (Figure 6A). Moreover, western blot data using biglycan and versican antibodies revealed that palmitate increased biglycan in the medium, whereas versican was minimally detected (Figure 6B). Interestingly, we found biglycan expression to be profoundly increased in thioglycollate-elicited peritoneal macrophages (Figures 6C and 6D).

To determine possible pathophysiological roles for macrophage-derived biglycan in adipose tissue inflammation, purified biglycan and biglycan-containing conditioned medium from palmitate-treated RPMs was added to 3T3-L1 adipocytes. Purified biglycan (Figure 6E) and conditioned medium from peritoneal macrophages exposed to palmitate (Figure 6F) increased the expression of *Saa3*, *Ccl2*, *Il1b*, and *Il6* in adipocytes. Moreover, when biglycan expression in macrophages was silenced with biglycan-specific siRNA, conditioned medium from biglycan-silenced macrophages partially ameliorated the expression of these genes in adipocytes (Figure 6F), suggesting an important role of macrophage-derived biglycan in regulating inflammation in adipocytes. We also found that purified biglycan increased NF-κB activation and decreased insulin signaling in adipocytes *in vitro* (Figures S6C and S6D). Collectively, these results suggest that biglycan-mediated crosstalk between adipocytes and macrophages plays a role in inflammation in adipose tissue.

DISCUSSION

In this study, we demonstrated that production of versican in adipose tissue from obese mice is largely confined to adipocytes, whereas production of biglycan is largely confined to macrophages. Specific deletion of versican from adipocytes reduced accumulation of macrophages and inflammatory gene expression in adipose tissue. Adipocyte-specific versican deletion also reduced liver inflammation and led to modestly improved insulin sensitivity and glucose tolerance. Macrophage-specific biglycan deletion also reduced adipose tissue macrophages and inflammatory gene expression but had no effect on the liver and did not lead to sustained improvement in insulin sensitivity and glucose tolerance. *In vitro* studies provided evidence of crosstalk between adipocytes and macrophages that involved versican and biglycan, suggesting that their interaction in adipose tissue modulates inflammation and insulin resistance.

To date, studies of the ECM in adipose tissue have focused mainly on alterations in collagen during development of obesity (Khan et al., 2009; Spencer et al., 2011; Sun et al., 2014). Collagen deficiency reduces adipose tissue inflammation in diet-induced obesity in mice

(Khan et al., 2009; Spencer et al., 2011; Sun et al., 2014), which suggests that collagen causes mechanical stress that constrains triglyceride storage. These findings are consistent with a role of collagen in forming a structural scaffold that regulates adipose tissue inflammation. Our findings in the present study indicate that the proteoglycans versican and biglycan, produced by adipocytes and macrophages, respectively, affect adipose tissue inflammation mainly by acting as bio-activators of inflammation. Separation of whole adipose tissue into AE and SVC fractions provides strong evidence that adipose tissue versican is derived predominantly from adipocytes, whereas the major cell source of biglycan is adipose tissue macrophages. Our findings, using human adipose tissue obtained at the time of bariatric surgery, are consistent with these data in that both proteoglycans were observed by gene expression and immunohistochemistry together with high levels of expression of other inflammatory genes. Because of the difficulty of obtaining omental adipose tissue from non-obese control subjects, we compared proteoglycans, chemokines, and cytokines in omental versus subcutaneous fat in obese individuals. Subcutaneous adipose tissue has been shown to have less inflammation and macrophage accumulation than visceral fat (Cancello et al., 2006; Harman-Boehm et al., 2007; Wajchenberg, 2000), which is consistent with our findings. Moreover, versican and biglycan were also increased in omental compared with subcutaneous fat. We were unable to separate the human samples into AE and macrophage-enriched fractions as we did with the mouse samples.

Versican is a large chondroitin sulfate proteoglycan produced by several cell types. Earlier studies demonstrated that 3T3-L1 pre-adipocytes increase their synthesis and secretion of versican when differentiating into adipocytes (Zizola et al., 2007). However, little is known about versican's role in adipose tissue or its involvement in obesity. Previously, we showed that a chondroitin sulfate-containing proteoglycan is produced by hypertrophic adipocytes *in vitro* and is present in adipose tissue from obese but not lean mice (Han et al., 2007, 2016). The presence of this proteoglycan blunted the anti-inflammatory properties of HDL by trapping SAA present in HDL in inflammatory states at the adipocyte cell surface (Han et al., 2016). In the present study, we identified this proteoglycan as versican. Specific deletion of versican expression in adipocytes has provided new insights into its role during development of obesity. Adipocyte-specific deletion of versican expression did not affect adipocyte differentiation or weight gain in response to the obesogenic diet but resulted in a reduction in adipose tissue macrophage content and inflammatory gene expression as well as reduced inflammation in the liver and improved insulin sensitivity and glucose tolerance to a similar extent as what has been found in other studies that showed improvement in these metabolic parameters in the absence of weight loss (Dobrian et al., 2013; Ke et al., 2015; Kitade et al., 2012; Liu et al., 2015; Macdougall et al., 2019; Park et al., 2016; Takei et al., 2019; Weisberg et al., 2006). The reason why adipocyte-specific deletion of versican led to reductions in liver inflammation and insulin resistance may relate to the increase in adiponectin and reduction in cytokine secretion from adipocytes. These findings support a major role of versican in regulating inflammation in adipose tissue in obesity, similar to its effects on inflammation in other tissues (Kang et al., 2017; Wight et al., 2014). For example, it interacts with other components in the ECM to form scaffolds that promote invasion, adhesion, and activation of immune and inflammatory leukocytes.

However, the mechanism by which versican might promote inflammation in adipose tissue remains speculative at this time. Our finding that exposure of 3T3-L1 adipocytes to high-glucose conditions shifted the differential sulfation patterns of the attached CS/DS-GAGs and to favor the 6S-CS branch of CS isomer sulfate modifications offers one such explanation. Sulfated GAG attachments are predicted to interact with a wide range of biologically active molecules (Hatano and Watanabe, 2020; Zhang et al., 2019), and binding studies show that the 6S-CS isomer enhances matrix binding to positively charged extracellular proteins over the 4S-CS isomer (Wight et al., 2014). Thus, the interactions between versican with pro- and anti-inflammatory regulators such as cytokines, lipoproteins, and proteases may be largely influenced by our reported change in the CS/DS-GAG sulfation pattern. An increase in the 6S-CS-to-4S-CS ratio of GAGs has been shown in arterial smooth muscle cells stimulated with platelet-derived growth factors (Cardoso et al., 2010; Schönherr et al., 1991) and in a number of cancers (Pude1ko et al., 2019), and 6S-CS has been suggested to have a greater binding potential to basic residues in cytokines and lipoproteins (Hurt-Camejo et al., 1992; Pichert et al., 2012; Pude1ko et al., 2019). The mechanisms by which versican CS/DS-GAG interactions might promote inflammation in adipose tissue in a physiological setting remains to be determined and warrants further investigation.

In vitro experiments demonstrated that conditioned medium from hypertrophic adipocytes activated chemokine and cytokine gene expression in recipient RPMs. However, neither addition of purified versican nor silencing of versican expression in adipocytes prior to collecting conditioned medium affected the expression of cytokines and chemokines in recipient quiescent macrophages. However, silencing versican in adipocytes reduced monocyte adhesion to hypertrophic adipocytes. These findings suggest that versican is responsible for sequestering monocytes and/or macrophages and that other factors, such as chemokines and cytokines produced by adipocytes but not versican, were responsible for stimulating inflammatory gene expression in quiescent macrophages.

One possible compound that might contribute to macrophage activation is versikine, a bioactive cleavage product of versican that acts as a damage-associated molecular pattern (DAMP). Versikine has been shown to stimulate pro-inflammatory downstream effects, such as activation of TLR2 signaling cascades, in macrophages and dendritic cells (Hope et al., 2016, 2017; Schmitt, 2016; Tang et al., 2015). Consistent with these effects of versikine, we found that purified versikine or versikine isolated after activated macrophages cleaved versican to this smaller product stimulated the expression of inflammatory genes in quiescent RPMs. Moreover, our findings showed that versikine activates NF-κB pathways and reduces insulin signaling in RPMs. However, conditioned medium from adipocytes in which versican, the precursor of versikine, had been silenced had a similar effect on recipient quiescent macrophage gene expression as conditioned medium from adipocytes in which versican had not been silenced. It is possible that macrophage activators produced by non-silenced adipocytes masked the effect of any versikine that was later formed by cleavage of versican by the newly activated macrophages. Thus, it is hard to determine the distinct effect of versikine in conditioned medium from the silencing experiments. Nonetheless, our findings imply that versikine is capable of stimulating inflammatory gene

expression and reducing insulin sensitivity in quiescent macrophages and that quiescent recipient macrophages do not cleave versican into versikine.

We also have shown that hypertrophic adipocytes produce a major versican binding partner, hyaluronan (Han et al., 2007). Hyaluronan (HA) is a simple non-sulfated glycosaminoglycan that lacks a core protein and is produced at the cell surface by one of 3 synthases: Has1–Has3. Has2 is upregulated in hypertrophic adipocytes so that HA accumulates in obese adipose tissue, where it binds macrophages and contributes to inflammation (Han et al., 2007). Binding of versican to HA generates an ECM with enhanced inflammatory cell binding properties, and modulation of either molecule regulates levels of tissue inflammation (Kang et al., 2017; Wight et al., 2014). Moreover, blocking versican with antibodies targeting HA-binding regions of the protein or by gene deletion led to a significant reduction in HA accumulation and, subsequently, HA-dependent monocyte adhesion (Kang et al., 2017; Potter-Perigo et al., 2010). Consistent with these observations, our study found that silencing versican in adipocytes decreased monocyte binding to the ECM, suggesting destabilization of HA in the ECM, which is the binding site of monocytes and macrophages via CD44 (de La Motte et al., 1999). Our findings thus suggest that versican provides a stabilizing scaffold for HA, creating a hydrated polyanionic environment favorable for leukocyte adhesion around inflamed adipocytes.

Moreover, under inflammatory conditions, HA is also broken down into fragments that, like versikine, act as DAMPs to activate TLR2 and/or TLR4-mediated inflammatory effects (Avenoso et al., 2019). Although the evidence clearly demonstrates that HA breakdown products can modulate stages of inflammation, the mechanism by which these HA fragments act is not completely understood. It is plausible that increased HA production by hypertrophic adipocytes leads to enhanced HA breakdown and that these HA fragments are a component in the conditioned medium with macrophage-stimulatory capability. Further investigation is needed to determine whether such fragments are generated and how they might contribute to the proinflammatory ECM generated by obese adipose tissue.

Biglycan is a small leucine-rich proteoglycan present in the ECM that acts as a DAMP (Frevert et al., 2018; Schaefer et al., 2005). Under physiological conditions, it is sequestered in the ECM. In injury and inflammation, biglycan can be synthesized by macrophages and cleaved proteolytically to generate soluble biglycan, which can bind TLR2/4, activating several inflammatory signaling pathways, such as NF-κB and mitogen-associated protein kinase (MAPK) pathways (Hsieh et al., 2017; Roedig et al., 2019a; Schaefer et al., 2005) and concomitantly triggering synthesis and secretion of a number of pro-inflammatory cytokines (Frevert et al., 2018; Frey et al., 2013; Nastase et al., 2012; Roedig et al., 2019b). Elevated biglycan levels are associated with inflammation, obesity, and type 2 diabetes (Bolton et al., 2012; Kim et al., 2016). Biglycan also has been implicated in insulin resistance in rodents (Kim et al., 2016), and global deletion of biglycan in diet-induced obese mice has been shown to lower adipose tissue inflammation in EWAT and improve glucose tolerance after 8 weeks of a high-fat diet (Adapala et al., 2012). The present study extends these findings in that chimeric mice in which biglycan was deleted in hematopoietic cells by transplanting bone marrow cells from mice globally deficient in biglycan gained weight to the same extent as control mice when fed the HFHS diet. Although adipose tissue

macrophage content was reduced and inflammatory gene expression blunted in adipose tissue, no anti-inflammatory changes were demonstrated in the liver, which differs from what was seen with adipocyte-specific versican deletion. Despite a considerable reduction in adipose tissue macrophages, insulin and glucose tolerance were only transiently improved after 8 weeks on the HFHS diet, similar to what has been shown with global biglycan deletion (Adapala et al., 2012), but reverted to being similar to control mice after 16 weeks. Increased lipolysis could lead to elevations in plasma levels of NEFA, which, in turn, could induce insulin resistance (Boden, 2003; I S Sobczak et al., 2019). However, fasting plasma levels of NEFA were actually decreased in macrophage-specific biglycan-deficient mice, whereas NEFA values in adipocyte-specific versican knockout mice did not differ from control mice, suggesting that the improved metabolic parameters in versican knockout mice compared with biglycan knockout mice were not due to increased lipolysis with a concomitant increases in plasma NEFA levels. Another possible explanation is that hepatic inflammation is a more important driver of insulin resistance than adipose tissue inflammation, as suggested by others (Burhans et al., 2018; Klein et al., 2007). Because the donor mice were CD45.2-positive and the recipient mice CD45.1-positive, it was possible to distinguish the source of macrophages present in the liver. Although nearly all macrophages in adipose tissue originated from the donor, a substantial portion of hepatic macrophages remained from the recipient. The transient effect of macrophage-specific biglycan deletion on glucose tolerance might relate to the observation that resident macrophages, likely Kupffer cells, were still present in the liver of recipient mice after irradiation, confounding the effect of macrophage biglycan deficiency in the liver. Future studies using a macrophage-specific biglycan deficiency model based on crossing LysM-Cre and biglycan-floxed mice might help address this question. Also, different from what we observed when silencing versican expression in adipocytes *in vitro*, silencing biglycan in cultured macrophages did reduce activation of gene expression in adipocytes exposed to macrophage-conditioned medium, implying a direct role of biglycan in influencing adipocyte inflammation but not necessarily insulin resistance.

In conclusion, adipocyte-derived versican and macrophage-derived biglycan play a pivotal role in adipose tissue inflammation in human and animal models of obesity. The findings from this study offer translational implications related to possibilities where modulation of ECM could be a therapeutic target to prevent obesity-associated complications.

STAR★METHODS

RESOURCE AVAILABILITY

Lead Contact—Further information and requests for resources and reagents should be directed to and will be fulfilled by the Lead Contact, Dr. Alan Chait (achait@uw.edu).

Materials Availability—*Adipoq-Cre/+;Vcan*$^{Flox/Flox}$ mouse line and recombinant versikine generated in this study are available from the Lead Contact with a completed Materials Transfer Agreement. We are glad to share those with reasonable compensation by requestor for its processing and shipping.

Data and Code Availability—This study did not generate new datasets or codes.

EXPERIMENTAL MODELS AND SUBJECT DETAILS

Animals and cell lines—All mice including C57BL/6 mice (Jackson Laboratory), *Adipoq-Cre/+;Vcan*$^{Flox/Flox}$ and *Adipoq-Cre/+;Vcan*$^{+/+}$, *Bgn*$^{-/0}$ and *Bgn*$^{+/0}$ (3–5 mice per cage, if not specially indicated) were housed in a temperature-controlled (21 ± 1.1°C), specific-pathogen free (SPF) facility under standard laboratory conditions (12 hours on/off; lights on at 7:00 a.m.) with food and water available *ad libitum*. Littermate control mice were used for all *in vivo* experiments. We used 10 week-old male mice, because they are more prone than females to the development of visceral obesity, adipose tissue inflammation and insulin resistance in response to a high-fat diet (Grove et al., 2010; Pettersson et al., 2012; Stubbins et al., 2012a, 2012b). Moreover, because the *Bgn* gene is located on the X chromosome (Chatterjee et al., 1993; McBride et al., 1990), male mice were used to generate chimeric mice in which *Bgn* is specifically deleted in myeloid cells (see later). Water and cages were autoclaved and cages were changed weekly, and the health status of the mice was monitored by The Rodent Health Monitoring Program (RHMP) at the University of Washington and the Benaroya Research Institute. All experimental procedures were undertaken with approval from the Institutional Animal Care and Use Committee of the University of Washington (Protocol #s 3104–01 and 4237–01) and Committee of the Benaroya Research Institute (Protocol # 16–024).

3T3-L1 murine pre-adipocytes (ATCC), human pre-adipocytes from Simpson-Golabi-Behmel syndrome (SGBS) were cultured in DMEM (Hyclone) containing 10% FBS (Hyclone). Pre-adipocytes were isolated from the stromal vascular fraction of collagenase-digested EWAT from *Adipoq-Cre/+;Vcan*$^{Flox/Flox}$ and *Adipoq-Cre/+;Vcan*$^{+/+}$ mice and grown in DMEM media (Hyclone) containing 10% FBS (Hyclone). Bone marrow-derived macrophages (BMDMs) isolated from the tibias and fibulas of C57BL/6 mice were cultured in RPMI 1640 media (Hyclone) containing 10% FBS (Hyclone). Thioglycollate (TG)-elicited peritoneal macrophages and RPM were obtained from the peritoneal cavities from several mouse strains and cultured in RPMI 1640 media (Hyclone) containing 10% FBS (Hyclone).

Human subjects—To investigate proteoglycans in adipose tissue from human subjects, subcutaneous and omental fat pads were isolated from obese subjects undergoing gastric-bypass surgery (18 females, 6 males, 45.41 ± 13.0 years of age (mean ± SD) and BMI of 40 or greater (n =24). All tissues were obtained through the UW Weight Disorders Clinic and processed in the core laboratories of the University of Washington's Nutrition Obesity Research Center. Human adipose tissues from 13 subjects were snap-frozen in liquid nitrogen and stored at −80°C. Samples from all 24 subjects were fixed with 10% neutral-buffered formalin and embedded in paraffin wax. All patients provided written informed consent and authorization for tissue biopsy, blood draws and release of medical information (Protocol #00002737).

METHOD DETAILS

Generation of obesity in animal models—To investigate the role of specific proteoglycans produced in adipose tissue during the development of obesity, we fed 10 week-old male C57BL/6 mice (Jackson Laboratory) either a high fat, high sucrose diet

(HFHS, 35.5% calories as fat and 36.6% as carbohydrate, 0.15% added cholesterol, BioServ No.F4997), which results in obesity, insulin resistance, and both adipose tissue and systemic inflammation (Subramanian et al., 2008), or a chow (control) diet for up to 16 weeks (n = 5 per group). At sacrifice, epididymal white adipose tissue (EWAT) was digested with collagenase (Worthington) (Montes et al., 2013), and the pelleted stromal vascular cells (SVC) were separated from the floating cells, i.e., the adipocyte-enriched (AE) fraction. To isolate the macrophage-enriched fraction, we performed magnetic immunoaffinity isolation with an anti-CD11b antibody conjugated to magnetic beads (MACS; Miltenyi Biotec) on SVC fractions (Cho et al., 2014). To determine whether macrophages were present in the AE fractions, we measured macrophage markers using RT-PCR. *F4/80* or *Cd11b*, macrophage markers, were minimally expressed, while *Adipoq* was highly expressed in AE fractions (data not shown). Cells were isolated using positive selection columns prior to preparation of whole-cell lysates.

To investigate the pathophysiological relevance of adipocyte-derived versican in the HFHS diet-induced model of obesity, we crossed an adiponectin-Cre transgenic mouse on a C57BL/6 background (*Adipoq-Cre*, a kind gift from Dr. Philip Scherer, University of Texas Southwestern) with a versican floxed mouse ($Vcan^{Flox/Flox}$) on a C57BL/6 background to obtain the $Adipoq\text{-}Cre/+;Vcan^{Flox/Flox}$ mice. Ten-week-old males of each genotype [$Adipoq\text{-}Cre/+;Vcan^{Flox/Flox}$ and $Adipoq\text{-}Cre/+;Vcan^{+/+}$ (controls)] were fed a HFHS for the indicated time periods (n = 10–12 per group). Body weights were measured weekly. Intra-peritoneal glucose (GTT) and insulin (ITT) tolerance tests were performed after a 4-hour fast as described previously (Subramanian et al., 2008), with insulin measured at 30 minutes during the GTT at 14 weeks (GTT) and 15 weeks (ITT). At euthanasia, harvested tissues were snap-frozen in liquid nitrogen and stored at − 70°C or were fixed with 10% neutral-buffered formalin (Fisher) and embedded in paraffin wax.

To investigate the pathophysiological role of macrophage-derived biglycan in HFHS diet-induced obesity, we generated chimeric mice in which biglycan is specifically deleted in myeloid cells. Since the *Bgn* gene is on the X chromosome (Chatterjee et al., 1993; McBride et al., 1990), male mice only have one copy. Thus, we chose to use male mice since it is easier to generate bone marrow-derived chimeric *Bgn*-deficient mice in males than females. For these experiments, whole bone marrow cells from male C57BL/6 and the global biglycan-deficient male mice ($Bgn^{-/0}$, on a C57BL/6 background, CD45.2 isotype) (Xu et al., 1998) were prepared by flushing the marrow cavities of femurs with PBS. Bone marrow cells ($5\ 3\ 10^6$) from littermate donor mice were injected retro-orbitally into recipient male C57BL/6 (CD45.1 isotype, Charles River) mice at 10 weeks of age, which had received irradiation (1000 rads) on the previous day. After a 2-week recovery period, C57BL/6 mice transplanted with marrow cells from $Bgn^{+/0}$ (n = 7) or $Bgn^{-/0}$ (n = 8) were fed a HFHS diet for 16 weeks (Averill et al., 2011; Gough and Raines, 2003). Body weights were measured weekly. Intra-peritoneal GTT was performed at 8 and 15 weeks after the onset of a HFHS diet, and ITT was performed after 16 weeks on the HFHS diet.

Real-time quantitative reverse-transcription polymerase chain reaction (RT-PCR)—Total RNA was isolated from the indicated adipose tissues and 2 mg was reverse transcribed into cDNA. RT-PCR was performed using the TaqMan Master kit (Thermo

Fisher Scientific) in the ABI prism 7900HT system (Han et al., 2006; Subramanian et al., 2008). Mouse and human primers with FAM probes were obtained from Thermo Fisher Scientific and are listed in Table S2. Each sample was analyzed in triplicate and normalized using *Gapdh* as control. Some samples also were normalized with a second housekeeping gene, b-2-microglobulin (*B2m*) and showed similar results.

Immunohistochemistry—For immunohistochemistry, adipose tissue was fixed in 10% formalin for immunohistochemical staining with antibodies against CD68 (Agilent, 1:200), Mac2 (R&D, 1:25), versican (Millipore, 1:250), biglycan (Thermo Fisher Scientific, 1:200), perlecan (Thermo Fisher Scientific, 1:250) and decorin (Thermo Fisher Scientific, 1:200), and photographed as described previously (O'Brien et al., 2005). Area quantification for each staining was performed on digital images of immunostained tissue sections using Image Pro Plus 6.0 (Media Cybernetics).

Genotyping—For genotyping, duplex PCR was performed on tail biopsies to distinguish WT and *Vcan Flox* alleles with WT-specific primers (IDT, forward 5′-CAGCCTGAGCAACAGGCACC-3′, reverse 5′-CCCTCTCGGGGAGCCCGTATG-3′) and LoxP-specific primers (forward 5′-AGAGCAGCTGTTTGCCGCCT-3′, reverse 5′-CCCTCTCGGGGAGCCCGTATG-3′). The resulting WT fragment is 763 bp, and the LoxP fragment is 391 bp.

Plasma analyses—Plasma was collected at the indicated time points following a 4-hour fast. Insulin and adiponectin were quantified using commercially available ELISA kits (EMD Millipore). SAA (R&D), total cholesterol (Stanbio) and triglycerides (Stanbio) were measured using ELISA (SAA) and colorimetric assays, as described previously (den Hartigh et al., 2014). Fasting non-esterified fatty acid (NEFA) was measured using the NEFA-C (Wako) according to the manufacturer's instructions.

Adipocyte differentiation from pre-adipocytes—Pre-adipocytes were isolated from the stromal vascular fraction of collagenase-digested EWAT from *Adipoq-Cre/+;Vcan*$^{Flox/Flox}$ and *Adipoq-Cre/+;Vcan*$^{+/+}$ mice, grown to confluency, and differentiated in DMEM media (Hyclone) containing 32 μmol/L dexamethasone (Sigma), 780 μmol/L 3-isobutyl-1-methylxanthine (Sigma), 10 μg/mL bovine insulin (Sigma), 1 μmol/L rosiglitazone (Cayman Chemical) and 1 μmol/L indomethacin (Sigma) for 4 days. Differentiated adipocytes were cultured for 7 days with daily replenishment of DMEM media. To confirm the extent of adipocyte differentiation from pre-adipocytes, total neutral lipid content of cells was visualized by staining with HCS LipidTOX (Invitrogen) and photographed using Image Pro Plus 6.0 (Media Cybernetics).

FACS analysis—Splenocytes were isolated from spleens of bone marrow chimeric mice by homogenization on 70 μm mesh cell strainers on tissue culture plates, followed by washing in RPMI media and incubating in ACK RBC lysis buffer (Thermo Fisher Scientific) for 4 minutes at 37°C to remove red blood cells. Cells were incubated with NIR Zombie (1:200, Biolegend) in PBS for live/dead staining for 15 minutes at room temperature, followed by PE CD45.1 (1:200, clone A20, eBioscience), APC CD45.2 (1:200, clone 104, Biolegend), BV 605 CD3e (1:200, clone 145–2C11, Biolegend), BV 650 CD19 (1:200,

clone 6D5, Biolegend), FITC CD11b (1:100, clone M1/70, eBioscience), Percp Cy5.5 Ly6G/Gr-1 (1:200, clone RB6–8C5, eBioscience), eFluor 450 F4/80 (1:200, clone BM8, eBioscience) and Fc blocker (1:100, anti-mouse CD16/32,BD) at 4°C in the dark for 20 minutes, and washed in PBS/0.5% BSA. Analysis was performed using an LSRII (Becton Dickinson) flow cytometer and FlowJo. v10 (Treestar).

Bone marrow-derived macrophages (BMDMs)—Bone marrow-derived macrophages (BMDMs) isolated from the tibias and fibulas of C57BL/6 mice were pooled and plated on 6-well plates in RPMI 1640 media (Hyclone) containing 10% FBS (Hyclone) and 30% L929 conditioned media (Vats et al., 2006). Medium was replaced on days 2 and 4 (with retention of floating and attached cells) and on day 6, when floating cells were discarded. To induce M1 or M2 phenotypes, on day 7 BMDMs were stimulated for 24 hours with IFN-γ (10 ng/mL; R&D Systems) and LPS (1 ng/mL; Cayman Chemical), or for 48 hours with IL4 (10 ng/mL; R&D Systems), respectively.

Cell culture—3T3-L1 murine pre-adipocytes (ATCC), human pre-adipocytes from Simpson-Golabi-Behmel syndrome (SGBS) were propagated and differentiated according to standard procedures (Yeop Han et al., 2010; Lin et al., 2005), except that cells were differentiated and propagated in DMEM containing 5 or 25 mmol/L glucose (Hyclone), and media were changed daily.

Thioglycollate (TG)-elicited peritoneal macrophages and RPM were obtained from the peritoneal cavities from several mouse strains. To obtain resident macrophages, PBS was injected intraperitoneally, and cells were collected immediately. To obtain TG-elicited macrophages, thioglycollate (BD) was injected intraperitoneally and cells were collected after 4 days. To remove non-adherent peritoneal cells from resident and TG-elicited peritoneal macrophages, the plates were washed extensively after adherence of macrophages to the plates for 60 minutes.

Palmitate (16:0) (Sigma) was conjugated with albumin, as described previously (Yeop Han et al., 2010). Briefly, palmitate was first dissolved in NaOH (100 mmol/L) and conjugated with fatty acid-free albumin (Sigma) at a molar ratio of 3:1 (palmitate/albumin).

3T3-L1 CS/DS-GAG isolation and LC-MS/MS + MRM sulfation analysis—3T3-L1 cells were grown in low (5 mmol/L) and high (25 mmol/L) glucose conditions for 7 days. CS/DS-GAG isolation and quantification were performed as previously described with slight adaptations for cell culture (Alonge et al., 2019). Briefly, after glucose treatment media was removed and cells were washed with 0.1 mol/L PBS and then fixed in 4% paraformaldehyde (Sigma) in 0.1 mol/L PBS for 6 days at 4°C. After fixation, the paraformaldehyde fixative was removed and GAGs were prepared for enzymatic digestion by 3 × washes in Optima LC-grade water (Fisher) and 1 × wash in 10 mmol/L ammonium bicarbonate (Sigma, pH 7.6). Digestion of GAGs occurred in 0.5 U/mL of chondroitin ABC lyase in 10 mM ammonium bicarbonate (pH 7.6) rocking at 37°C for 24 hours. CS/DS disaccharides were isolated, purified, and analyzed using an ultra-performance liquid chromatographic system (UPLC) system coupled to a triple quadrupole mass spectrometer equipped with an electrospray ion source as previously described (Alonge et al., 2019; Osago et al., 2014), and

MRM channels were assigned as: Δ4S-CS *m/z* 458 > 300, Δ4S6S-CS and Δ2S4S- ΔS *m/z* 538 > 300, Δ0S-CS and ΔHA *m/z* 378 > 175, Δ6S-C S *m/z* 458 > 282, and Δ2S6S-CS *m/z* 268 > 282. MassLynx was used to acquire and quantify all data and the relative quantification of each CS/DS isomer within a sample was computed using a modified peak area normalization function (Alonge et al., 2019; Yu et al., 2014). As such, each CS/DS isomer is expressed as a relative percentage of the total CS/DS isomer composition within a 3T3-L1 sample.

***In vitro* versican and biglycan gene silencing—**For experiments in which we tested the roles of versican and biglycan in mediating crosstalk between adipocytes and macrophages, 3T3-L1 adipocytes and TG-elicited peritoneal macrophages were transiently transfected with small interfering RNA (siRNA) duplexes for versican and biglycan or scrambled sequences, which were synthesized and purified by Ambion using the DeliverX system (Panomics), as described previously (Yeop Han et al., 2010).

Recombinant versikine production—Recombinant versikine was generated by modifying an existing recombinant production system generated previously (Foulcer et al., 2015). Briefly, consensus coding nucleotides 831–1679 of human V1 versican with C-terminal Twin-Strep-Tag® and flanking XbaI and BamHI restriction enzyme sites was spliced onto upstream sequence of the common versican G1 domain sequence residing in a lentiviral vector developed for generating large quantities of recombinant mammalian proteins utilizing an ubiquitous chromatin opening element (Bandaranayake et al., 2011). This was further modified to include a matrix attachment region and stabilizing anti-repressor element. Secreted versikine generated by stably-transduced HEK293T/17 SF cells (ATCC), was purified from serum-free conditioned media (Sigma) using a Strep-Tactin® resin column (IBA). Purified versikine was validated by Coomassie staining and western blot (see Figure S5) using an antibody against the versican cleavage neo-epitope (DPEAAE) (Thermo Fischer Scientific, 1:1000).

Western blot analysis—Culture media from 3T3-L1 adipocytes, TG-elicited macrophages and resident macrophages were analyzed by western blot using anti-versican, biglycan, perlecan and decorin antibodies. Media samples were concentrated and purified by ion-exchange chromatography on diethylaminoethyl (DEAE) Sephacel (Sigma) in 8 mol/L urea buffer (8 mol/L urea, 2 mmol/L EDTA, 50 mmol/L Tris base,0.25 mol/L NaCl, 0.5% TX-100, pH 7.5). The columns were washed with 8 mol/L urea buffer and eluted with 8 mol/L urea buffer containing 2 mol/L NaCl. Samples were ethanol precipitated and digested with chondroitin ABC lyase (Sigma) for 3 hours at 37°C. The samples were reduced and electrophoresed on a 4%–12% gradient SDS-PAGE gel. Proteins were then transferred to nitrocellulose membranes using a Bio-Rad Transblot SD. Semi-Dry Transfer Cell. After incubation with the blocking buffer (10% Aqua Block, East-Coast Bio in TBS-T containing 0.1% Tween-20) for 2 hours at room temperature, membranes were incubated with a goat polyclonal antibody against mouse versican βGAG domain (Millipore, 1:1000), a rabbit polyclonal antibody against biglycan (Thermo Fisher Scientific, 1:1000), a rabbit polyclonal antibody against decorin (Thermo Fisher Scientific, 1:1000) and a rat monoclonal antibody against perlecan (Thermo Fisher Scientific,1:1000), respectively overnight at 4°C in

blocking buffer. TBS-T was used for all washing steps. After incubation with fluorescence-conjugated secondary antibody for 1 hour at room temperature, membranes were washed and scanned by using a LI-COR Odyssey® scanner and software (LI-COR Biotechnology).

Activation of NFκB and insulin signaling in 3T3-L1 adipocytes and resident macrophages after exposure of biglycan and versikine, respectively, were analyzed by western blot using anti-phosphorylated NFκB p65 (ser536, 1:1000) anti-total NFκB p65 antibodies (Cell Signaling, 1:1000), and anti-phosphorylated Akt (serine 473, Cell Signaling, 1:1000) and anti-total Akt rabbit polyclonal antibodies (Cell Signaling, 1:1000). After incubation with fluorescence-conjugated secondary antibody for 1 hour at room temperature, membranes were washed and scanned by using a LI-COR Odyssey® scanner and software (LI-COR Biotechnology).

Monocyte adhesion assay—Differentiated 3T3-L1 adipocytes were cultured for 7 days in 5 mmol/L or 25 mmol/L glucose. To examine how many monocytes attached to the cultured adipocytes, U937 cells (10^6 cells /mL, ATCC) were fluorescently labeled by incubation with calcein-AM (5 μg/mL, Molecular Probes) for 30–45 minutes, and washed twice in phenol red-free RPMI medium (GIBCO) (Yeop Han et al., 2010). Suspended U937 cells were then added to 3T3-L1 adipocyte monolayers and allowed to adhere for 90 minutes at 4°C. Plates were washed gently three times and visualized to ensure monolayer integrity, before measuring fluorescence in a FusionTM Series Universal Microplate Analyzer (Packard Bioscience) with excitation and detection wavelengths of 485 and 535 nm, respectively.

QUANTIFICATION AND STATISTICAL ANALYSIS

Statistical significance was determined with SPSS (Windows version 19) or OriginPro software (version 8.6; Origin Laboratory). All data are shown as means ± SEM. Student's t test was used to detect differences within groups when applicable (2-tailed). Oneway ANOVA (ANOVA) was used to compare differences among all groups, and Bonferroni post hoc testing was used to detect differences among mean values of the groups. A p value < 0.05 was considered statistically significant.

Supplementary Material

Refer to Web version on PubMed Central for supplementary material.

ACKNOWLEDGMENTS

This work was supported in part by National Institutes of Health, United States, grants HL092969 (to A.C.), AI125378, and AI130280 (to T.N.W.), and DK122662 (to K.M.A.). Part of the study was supported by the University of Washington Nutrition Obesity Research Center (DK035816). We would like to thank the Diabetes Program Project core service (Tomasz Wietecha) at the University of Washington (HL092969) and Pamela Y. Johnson, PhD, and the HistoCore at the Benaroya Research Institute for performing immunohistochemistry on adipose tissues. The mass spectrometry work was supported by the University of Washington School of Pharmacy Mass Spectrometry Center. We also thank Virginia M. Green, PhD, at BRI for careful editing of the manuscript.

REFERENCES

Adapala VJ, Ward M, and Ajuwon KM (2012). Adipose tissue biglycan as a potential anti-inflammatory target of sodium salicylate in mice fed a high fat diet J. Inflamm (Lond) 9, 15.

Alonge KM, Logsdon AF, Murphree TA, Banks WA, Keene CD, Edgar JS, Whittington D, Schwartz MW, and Guttman M (2019). Quantitative analysis of chondroitin sulfate disaccharides from human and rodent fixed brain tissue by electrospray ionization-tandem mass spectrometry. Glycobiology 29, 847–860. [PubMed: 31361007]

Avenoso A, Bruschetta G, D'Ascola A, Scuruchi M, Mandraffino G, Gullace R, Saitta A, Campo S, and Campo GM (2019). Hyaluronan fragments produced during tissue injury: A signal amplifying the inflammatory response. Arch. Biochem. Biophys 663, 228–238. [PubMed: 30668938]

Averill MM, Barnhart S, Becker L, Li X, Heinecke JW, Leboeuf RC, Hamerman JA, Sorg C, Kerkhoff C, and Bornfeldt KE (2011). S100A9 differentially modifies phenotypic states of neutrophils, macrophages, and dendritic cells: implications for atherosclerosis and adipose tissue inflammation. Circulation 123, 1216–1226. [PubMed: 21382888]

Babelova A, Moreth K, Tsalastra-Greul W, Zeng-Brouwers J, Eickelberg O, Young MF, Bruckner P, Pfeilschifter J, Schaefer RM, Gröne HJ, and Schaefer L (2009). Biglycan, a danger signal that activates the NLRP3 inflammasome via toll-like and P2X receptors. J. Biol. Chem 284, 24035–24048. [PubMed: 19605353]

Bandaranayake AD, Correnti C, Ryu BY, Brault M, Strong RK, and Rawlings DJ (2011). Daedalus: a robust, turnkey platform for rapid production of decigram quantities of active recombinant proteins in human cell lines using novel lentiviral vectors. Nucleic Acids Res. 39, e143. [PubMed: 21911364]

Boden G (2003). Effects of free fatty acids (FFA) on glucose metabolism: significance for insulin resistance and type 2 diabetes. Exp. Clin. Endocrinol. Diabetes 111, 121–124. [PubMed: 12784183]

Bolton K, Segal D, and Walder K (2012). The small leucine-rich proteoglycan, biglycan, is highly expressed in adipose tissue of Psammomys obesus and is associated with obesity and type 2 diabetes. Biologics 6, 67–72. [PubMed: 22532774]

Bulló M, García-Lorda P, Megias I, and Salas-Salvadó J (2003). Systemic inflammation, adipose tissue tumor necrosis factor, and leptin expression. Obes. Res 11, 525–531. [PubMed: 12690081]

Burhans MS, Hagman DK, Kuzma JN, Schmidt KA, and Kratz M (2018). Contribution of Adipose Tissue Inflammation to the Development of Type 2 Diabetes Mellitus. Compr. Physiol 9, 1–58. [PubMed: 30549014]

Cancello R, and Clément K (2006). Is obesity an inflammatory illness? Role of low-grade inflammation and macrophage infiltration in human white adipose tissue. BJOG 113, 1141–1147. [PubMed: 16903845]

Cancello R, Tordjman J, Poitou C, Guilhem G, Bouillot JL, Hugol D, Coussieu C, Basdevant A, Bar Hen A, Bedossa P, et al. (2006). Increased infiltration of macrophages in omental adipose tissue is associated with marked hepatic lesions in morbid human obesity. Diabetes 55, 1554–1561. [PubMed: 16731817]

Cardoso LE, Little PJ, Ballinger ML, Chan CK, Braun KR, Potter-Perigo S, Bornfeldt KE, Kinsella MG, and Wight TN (2010). Platelet-derived growth factor differentially regulates the expression and post-translational modification of versican by arterial smooth muscle cells through distinct protein kinase C and extracellular signal-regulated kinase pathways. J. Biol. Chem 285, 6987–6995. [PubMed: 20042606]

Chatterjee A, Faust CJ, and Herman GE (1993). Genetic and physical mapping of the biglycan gene on the mouse X chromosome. Mamm. Genome 4, 33–36. [PubMed: 8093671]

Chen J, Spagnoli A, and Torquati A (2012). Omental gene expression of adiponectin correlates with degree of insulin sensitivity before and after gastric bypass surgery. Obes. Surg 22, 472–477. [PubMed: 22161113]

Cho KW, Morris DL, and Lumeng CN (2014). Flow cytometry analyses of adipose tissue macrophages. Methods Enzymol. 537, 297–314. [PubMed: 24480353]

de La Motte CA, Hascall VC, Calabro A, Yen-Lieberman B, and Strong SA (1999). Mononuclear leukocytes preferentially bind via CD44 to hyaluronan on human intestinal mucosal smooth

muscle cells after virus infection or treatment with poly(I.C). J. Biol. Chem 274, 30747–30755. [PubMed: 10521464]

den Hartigh LJ, Wang S, Goodspeed L, Ding Y, Averill M, Subramanian S, Wietecha T, O'Brien KD, and Chait A (2014). Deletion of serum amyloid A3 improves high fat high sucrose diet-induced adipose tissue inflammation and hyperlipidemia in female mice. PLoS ONE 9, e108564. [PubMed: 25251243]

Divoux A, Tordjman J, Lacasa D, Veyrie N, Hugol D, Aissat A, Basdevant A, Guerre-Millo M, Poitou C, Zucker JD, et al. (2010). Fibrosis in human adipose tissue: composition, distribution, and link with lipid metabolism and fat mass loss. Diabetes 59, 2817–2825. [PubMed: 20713683]

Dobrian AD, Galkina EV, Ma Q, Hatcher M, Aye SM, Butcher MJ, Ma K, Haynes BA, Kaplan MH, and Nadler JL (2013). STAT4 deficiency reduces obesity-induced insulin resistance and adipose tissue inflammation. Diabetes 62, 4109–4121. [PubMed: 23939393]

Foulcer SJ, Day AJ, and Apte SS (2015). Isolation and purification of versican and analysis of versican proteolysis. Methods Mol. Biol 1229, 587–604. [PubMed: 25325983]

Frevert CW, Felgenhauer J, Wygrecka M, Nastase MV, and Schaefer L (2018). Danger-Associated Molecular Patterns Derived From the Extracellular Matrix Provide Temporal Control of Innate Immunity. J. Histochem. Cytochem 66, 213–227. [PubMed: 29290139]

Frey H, Schroeder N, Manon-Jensen T, Iozzo RV, and Schaefer L (2013). Biological interplay between proteoglycans and their innate immune receptors in inflammation. FEBS J. 280, 2165–2179. [PubMed: 23350913]

Gough PJ, and Raines EW (2003). Gene therapy of apolipoprotein E-deficient mice using a novel macrophage-specific retroviral vector. Blood 101, 485–491. [PubMed: 12393475]

Grove KL, Fried SK, Greenberg AS, Xiao XQ, and Clegg DJ (2010). A microarray analysis of sexual dimorphism of adipose tissues in high-fat-diet-induced obese mice. Int. J. Obes 34, 989–1000.

Han CY, Chiba T, Campbell JS, Fausto N, Chaisson M, Orasanu G, Plutzky J, and Chait A (2006). Reciprocal and coordinate regulation of serum amyloid A versus apolipoprotein A-I and paraoxonase-1 by inflammation in murine hepatocytes. Arterioscler. Thromb. Vasc. Biol 26, 1806–1813. [PubMed: 16709944]

Han CY, Subramanian S, Chan CK, Omer M, Chiba T, Wight TN, and Chait A (2007). Adipocyte-derived serum amyloid A3 and hyaluronan play a role in monocyte recruitment and adhesion. Diabetes 56, 2260–2273. [PubMed: 17563062]

Han CY, Tang C, Guevara ME, Wei H, Wietecha T, Shao B, Subramanian S, Omer M, Wang S, O'Brien KD, et al. (2016). Serum amyloid A impairs the antiinflammatory properties of HDL. J. Clin. Invest 126, 266–281. [PubMed: 26642365]

Harman-Boehm I, Blüher M, Redel H, Sion-Vardy N, Ovadia S, Avinoach E, Shai I, Klöting N, Stumvoll M, Bashan N, and Rudich A (2007). Macrophage infiltration into omental versus subcutaneous fat across different populations: effect of regional adiposity and the comorbidities of obesity. J. Clin. Endocrinol. Metab 92, 2240–2247. [PubMed: 17374712]

Hatano S, and Watanabe H (2020). Regulation of Macrophage and Dendritic Cell Function by Chondroitin Sulfate in Innate to Antigen-Specific Adaptive Immunity. Front. Immunol 11, 232. [PubMed: 32194548]

Hirose J, Kawashima H, Yoshie O, Tashiro K, and Miyasaka M (2001). Versican interacts with chemokines and modulates cellular responses. J. Biol. Chem 276, 5228–5234. [PubMed: 11083865]

Hope C, Foulcer S, Jagodinsky J, Chen SX, Jensen JL, Patel S, Leith C, Maroulakou I, Callander N, Miyamoto S, et al. (2016). Immunoregula-tory roles of versican proteolysis in the myeloma microenvironment. Blood 128, 680–685. [PubMed: 27259980]

Hope C, Emmerich PB, Papadas A, Pagenkopf A, Matkowskyj KA, Van De Hey DR, Payne SN, Clipson L, Callander NS, Hematti P, et al. (2017). Versican-Derived Matrikines Regulate Batf3-Dendritic Cell Differentiation and Promote T Cell Infiltration in Colorectal Cancer. J. Immunol 199, 1933–1941. [PubMed: 28754680]

Hsieh LT, Nastase MV, Roedig H, Zeng-Brouwers J, Poluzzi C, Schwalm S, Fork C, Tredup C, Brandes RP, Wygrecka M, et al. (2017). Biglycan- and Sphingosine Kinase-1 Signaling Crosstalk Regulates the Synthesis of Macrophage Chemoattractants. Int. J. Mol. Sci 18, 595.

Huber J, Löffler M, Bilban M, Reimers M, Kadl A, Todoric J, Zeyda M, Geyeregger R, Schreiner M, Weichhart T, et al. (2007). Prevention of high-fat diet-induced adipose tissue remodeling in obese diabetic mice by n-3 polyunsaturated fatty acids. Int. J. Obes 31, 1004–1013.

Hurt-Camejo E, Camejo G, Rosengren B, López F, Ahlström C, Fager G, and Bondjers G (1992). Effect of arterial proteoglycans and glycosaminoglycans on low density lipoprotein oxidation and its uptake by human macrophages and arterial smooth muscle cells. Arterioscler. Thromb 12, 569–583. [PubMed: 1576119]

I S Sobczak A, A Blindauer C, and J Stewart A (2019). Changes in Plasma Free Fatty Acids Associated with Type-2 Diabetes. Nutrients 11, 2022.

Ismail NA, Alavi MZ, and Moore S (1994). Lipoprotein-proteoglycan complexes from injured rabbit aortas accelerate lipoprotein uptake by arterial smooth muscle cells. Atherosclerosis 105, 79–87. [PubMed: 8155089]

Kang I, Harten IA, Chang MY, Braun KR, Sheih A, Nivison MP, Johnson PY, Workman G, Kaber G, Evanko SP, et al. (2017). Versican deficiency significantly reduces lung inflammatory response induced by polyino-sine-polycytidylic acid stimulation. J. Biol. Chem 292, 51–63. [PubMed: 27895126]

Kang I, Chang MY, Wight TN, and Frevert CW (2018). Proteoglycans as Immunomodulators of the Innate Immune Response to Lung Infection. J. Histochem. Cytochem 66, 241–259. [PubMed: 29328866]

Ke B, Zhao Z, Ye X, Gao Z, Manganiello V, Wu B, and Ye J (2015). Inactivation of NF-kB p65 (RelA) in Liver Improves Insulin Sensitivity and Inhibits cAMP/PKA Pathway. Diabetes 64, 3355–3362. [PubMed: 26038580]

Kern PA, Di Gregorio GB, Lu T, Rassouli N, and Ranganathan G (2003). Adiponectin expression from human adipose tissue: relation to obesity, insulin resistance, and tumor necrosis factor-alpha expression. Diabetes 52, 1779–1785. [PubMed: 12829646]

Khan T, Muise ES, Iyengar P, Wang ZV, Chandalia M, Abate N, Zhang BB, Bonaldo P, Chua S, and Scherer PE (2009). Metabolic dys-regulation and adipose tissue fibrosis: role of collagen VI. Mol. Cell. Biol 29, 1575–1591. [PubMed: 19114551]

Kim J, Lee SK, Shin JM, Jeoun UW, Jang YJ, Park HS, Kim JH, Gong GY, Lee TJ, Hong JP, et al. (2016). Enhanced biglycan gene expression in the adipose tissues of obese women and its association with obesity-related genes and metabolic parameters. Sci. Rep 6, 30609. [PubMed: 27465988]

Kitade H, Sawamoto K, Nagashimada M, Inoue H, Yamamoto Y, Sai Y, Takamura T, Yamamoto H, Miyamoto K, Ginsberg HN, et al. (2012). CCR5 plays a critical role in obesity-induced adipose tissue inflammation and insulin resistance by regulating both macrophage recruitment and M1/ M2 status. Diabetes 61, 1680–1690. [PubMed: 22474027]

Klein I, Cornejo JC, Polakos NK, John B, Wuensch SA, Topham DJ, Pierce RH, and Crispe IN (2007). Kupffer cell heterogeneity: functional properties of bone marrow derived and sessile hepatic macrophages. Blood 110, 4077–4085. [PubMed: 17690256]

Lin Y, Berg AH, Iyengar P, Lam TK, Giacca A, Combs TP, Rajala MW, Du X, Rollman B, Li W, et al. (2005). The hyperglycemia-induced inflammatory response in adipocytes: the role of reactive oxygen species. J. Biol. Chem 280, 4617–4626. [PubMed: 15536073]

Liu Y, Ge X, Dou X, Guo L, Liu Y, Zhou SR, Wei XB, Qian SW, Huang HY, Xu CJ, et al. (2015). Protein Inhibitor of Activated STAT 1 (PIAS1) Protects Against Obesity-Induced Insulin Resistance by Inhibiting Inflammation Cascade in Adipose Tissue. Diabetes 64, 4061–4074. [PubMed: 26324179]

Llorente-Cortés V, Otero-Viñas M, Hurt-Camejo E, Martínez-González J, and Badimon L (2002). Human coronary smooth muscle cells internalize versican-modified LDL through LDL receptor-related protein and LDL receptors. Arterioscler. Thromb. Vasc. Biol 22, 387–393. [PubMed: 11884279]

Maachi M, Piéroni L, Bruckert E, Jardel C, Fellahi S, Hainque B, Capeau J, and Bastard JP (2004). Systemic low-grade inflammation is related to both circulating and adipose tissue TNFalpha, leptin and IL-6 levels in obese women. Int. J. Obes. Relat. Metab. Disord 28, 993–997. [PubMed: 15211360]

Macdougall CE, Wood EG, Solomou A, Scagliotti V, Taketo MM, Gaston-Massuet C, Marelli-Berg FM, Charalambous M, and Longhi MP (2019). Constitutive Activation of β-Catenin in Conventional Dendritic Cells Increases the Insulin Reserve to Ameliorate the Development of Type 2 Diabetes in Mice. Diabetes 68, 1473–1484. [PubMed: 31048369]

Mariman EC, and Wang P (2010). Adipocyte extracellular matrix composition, dynamics and role in obesity. Cell. Mol. Life Sci 67, 1277–1292. [PubMed: 20107860]

McBride OW, Fisher LW, and Young MF (1990). Localization of PGI (biglycan, BGN) and PGII (decorin, DCN, PG-40) genes on human chromosomes Xq13-qter and 12q, respectively. Genomics 6, 219–225. [PubMed: 1968422]

Montes VN, Turner MS, Subramanian S, Ding Y, Hayden-Ledbetter M, Slater S, Goodspeed L, Wang S, Omer M, Den Hartigh LJ, et al. (2013). T cell activation inhibitors reduce CD8+ T cell and pro-inflammatory macrophage accumulation in adipose tissue of obese mice. PLoS ONE 8, e67709. [PubMed: 23844072]

Nastase MV, Young MF, and Schaefer L (2012). Biglycan: a multivalent proteoglycan providing structure and signals. J. Histochem. Cytochem 60, 963–975. [PubMed: 22821552]

O'Brien KD, McDonald TO, Kunjathoor V, Eng K, Knopp EA, Lewis K, Lopez R, Kirk EA, Chait A, Wight TN, et al. (2005). Serum amyloid A and lipoprotein retention in murine models of atherosclerosis. Arterioscler. Thromb. Vasc. Biol 25, 785–790. [PubMed: 15692094]

Osago H, Shibata T, Hara N, Kuwata S, Kono M, Uchio Y, and Tsuchiya M (2014). Quantitative analysis of glycosaminoglycans, chondroitin/dermatan sulfate, hyaluronic acid, heparan sulfate, and keratan sulfate by liquid chromatography-electrospray ionization-tandem mass spectrometry. Anal. Biochem 467, 62–74. [PubMed: 25197028]

Park SH, Liu Z, Sui Y, Helsley RN, Zhu B, Powell DK, Kern PA, and Zhou C (2016). IKKβ Is Essential for Adipocyte Survival and Adaptive Adipose Remodeling in Obesity. Diabetes 65, 1616–1629. [PubMed: 26993069]

Pettersson US, Waldén TB, Carlsson PO, Jansson L, and Phillipson M (2012). Female mice are protected against high-fat diet induced metabolic syndrome and increase the regulatory T cell population in adipose tissue. PLoS ONE 7, e46057. [PubMed: 23049932]

Pichert A, Samsonov SA, Theisgen S, Thomas L, Baumann L, Schiller J, Beck-Sickinger AG, Huster D, and Pisabarro MT (2012). Characterization of the interaction of interleukin-8 with hyaluronan, chondroitin sulfate, dermatan sulfate and their sulfated derivatives by spectroscopy and molecular modeling. Glycobiology 22, 134–145. [PubMed: 21873605]

Potter-Perigo S, Johnson PY, Evanko SP, Chan CK, Braun KR, Wilkinson TS, Altman LC, and Wight TN (2010). Polyinosine-polycytidylic acid stimulates versican accumulation in the extracellular matrix promoting monocyte adhesion. Am. J. Respir. Cell Mol. Biol 43, 109–120. [PubMed: 19717812]

Pude1ko A, Wisowski G, Olczyk K, and Koźma EM (2019). The dual role of the glycosaminoglycan chondroitin-6-sulfate in the development, progression and metastasis of cancer. FEBS J 286, 1815–1837. [PubMed: 30637950]

Roedig H, Nastase MV, Frey H, Moreth K, Zeng-Brouwers J, Poluzzi C, Hsieh LT, Brandts C, Fulda S, Wygrecka M, and Schaefer L (2019a). Biglycan is a new high-affinity ligand for CD14 in macrophages. Matrix Biol 77, 4–22. [PubMed: 29777767]

Roedig H, Nastase MV, Wygrecka M, and Schaefer L (2019b). Breaking down chronic inflammatory diseases: the role of biglycan in promoting a switch between inflammation and autophagy. FEBS J 286, 2965–2979. [PubMed: 30776184]

Schaefer L, Babelova A, Kiss E, Hausser HJ, Baliova M, Krzyzankova M, Marsche G, Young MF, Mihalik D, Götte M, et al. (2005). The matrix component biglycan is proinflammatory and signals through Toll-like receptors 4 and 2 in macrophages. J. Clin. Invest 115, 2223–2233. [PubMed: 16025156]

Schmitt M (2016). Versican vs versikine: tolerance vs attack. Blood 128, 612–613. [PubMed: 27492311]

Schönherr E, Järveläinen HT, Sandell LJ, and Wight TN (1991). Effects of platelet-derived growth factor and transforming growth factor-beta 1 on the synthesis of a large versican-like chondroitin

sulfate proteoglycan by arterial smooth muscle cells. J. Biol. Chem 266, 17640–17647. [PubMed: 1894644]

Snyder JM, Washington IM, Birkland T, Chang MY, and Frevert CW (2015). Correlation of Versican Expression, Accumulation, and Degradation during Embryonic Development by Quantitative Immunohistochemistry. J. Histochem. Cytochem 63, 952–967. [PubMed: 26385570]

Spencer M, Unal R, Zhu B, Rasouli N, McGehee RE Jr., Peterson CA, and Kern PA (2011). Adipose tissue extracellular matrix and vascular abnor malities in obesity and insulin resistance. J. Clin. Endocrinol. Metab 96, E1990–E1998. [PubMed: 21994960]

Srinivasan SR, Xu JH, Vijayagopal P, Radhakrishnamurthy B, and Berenson GS (1995). Low-density lipoprotein binding affinity of arterial chondroitin sulfate proteoglycan variants modulates cholesteryl ester accumulation in macrophages. Biochim. Biophys. Acta 1272, 61–67. [PubMed: 7662721]

Stubbins RE, Holcomb VB, Hong J, and Núñez NP (2012a). Estrogen modulates abdominal adiposity and protects female mice from obesity and impaired glucose tolerance. Eur. J. Nutr 51, 861–870. [PubMed: 22042005]

Stubbins RE, Najjar K, Holcomb VB, Hong J, and Núñez NP (2012b). Oestrogen alters adipocyte biology and protects female mice from adipocyte inflammation and insulin resistance. Diabetes Obes. Metab 14, 58–66. [PubMed: 21834845]

Subramanian S, Han CY, Chiba T, McMillen TS, Wang SA, Haw A 3rd, Kirk EA, O'Brien KD, and Chait A (2008). Dietary cholesterol worsens adipose tissue macrophage accumulation and atherosclerosis in obese LDL receptor-deficient mice. Arterioscler. Thromb. Vasc. Biol 28, 685–691. [PubMed: 18239153]

Sun K, Park J, Gupta OT, Holland WL, Auerbach P, Zhang N, Goncalves Marangoni R, Nicoloro SM, Czech MP, Varga J, et al. (2014). Endotrophin triggers adipose tissue fibrosis and metabolic dysfunction. Nat. Commun 5, 3485. [PubMed: 24647224]

Takei A, Nagashima S, Takei S, Yamamuro D, Murakami A, Wakabayashi T, Isoda M, Yamazaki H, Ebihara C, Takahashi M, et al. (2019). Myeloid HMG-CoA Reductase Determines Adipose Tissue Inflammation, Insulin Resistance, and Hepatic Steatosis in Diet-Induced Obese Mice. Diabetes 69, 158–164. [PubMed: 31690648]

Tang M, Diao J, Gu H, Khatri I, Zhao J, and Cattral MS (2015). Toll-like Receptor 2 Activation Promotes Tumor Dendritic Cell Dysfunction by Regulating IL-6 and IL-10 Receptor Signaling. Cell Rep 13, 2851–2864. [PubMed: 26711349]

Taylor KR, and Gallo RL (2006). Glycosaminoglycans and their proteoglycans: host-associated molecular patterns for initiation and modulation of inflammation. FASEB J 20, 9–22. [PubMed: 16394262]

Vats D, Mukundan L, Odegaard JI, Zhang L, Smith KL, Morel CR, Wagner RA, Greaves DR, Murray PJ, and Chawla A (2006). Oxidative metabolism and PGC-1beta attenuate macrophage-mediated inflammation. Cell Metab 4, 13–24. [PubMed: 16814729]

Wajchenberg BL (2000). Subcutaneous and visceral adipose tissue: their relation to the metabolic syndrome. Endocr. Rev 21, 697–738. [PubMed: 11133069]

Weisberg SP, McCann D, Desai M, Rosenbaum M, Leibel RL, and Ferrante AW Jr. (2003). Obesity is associated with macrophage accumulation in adipose tissue. J. Clin. Invest 112, 1796–1808. [PubMed: 14679176]

Weisberg SP, Hunter D, Huber R, Lemieux J, Slaymaker S, Vaddi K, Charo I, Leibel RL, and Ferrante AW Jr. (2006). CCR2 modulates inflammatory and metabolic effects of high-fat feeding. J. Clin. Invest 116, 115–124. [PubMed: 16341265]

Wellen KE, and Hotamisligil GS (2003). Obesity-induced inflammatory changes in adipose tissue. J. Clin. Invest 112, 1785–1788. [PubMed: 14679172]

Wight TN (2002). Versican: a versatile extracellular matrix proteoglycan in cell biology. Curr. Opin. Cell Biol 14, 617–623. [PubMed: 12231358]

Wight TN, Kang I, and Merrilees MJ (2014). Versican and the control of inflammation. Matrix Biol 35, 152–161. [PubMed: 24513039]

Wight TN, Kang I, Evanko SP, Harten IA, Chang MY, Pearce OMT, Allen CE, and Frevert CW (2020). Versican-A Critical Extracellular Matrix Regulator of Immunity and Inflammation. Front. Immunol 11, 512. [PubMed: 32265939]

Williams KJ, and Tabas I (1995). The response-to-retention hypothesis of early atherogenesis. Arterioscler. Thromb. Vasc. Biol 15, 551–561. [PubMed: 7749869]

Williams KJ, and Tabas I (1998). The response-to-retention hypothesis of atherogenesis reinforced. Curr. Opin. Lipidol 9, 471–474. [PubMed: 9812202]

Wu YJ, La Pierre DP, Wu J, Yee AJ, and Yang BB (2005). The interaction of versican with its binding partners. Cell Res 15, 483–494. [PubMed: 16045811]

Xu T, Bianco P, Fisher LW, Longenecker G, Smith E, Goldstein S, Bonadio J, Boskey A, Heegaard AM, Sommer B, et al. (1998). Targeted disruption of the biglycan gene leads to an osteoporosis-like phenotype in mice. Nat. Genet 20, 78–82. [PubMed: 9731537]

Xu H, Barnes GT, Yang Q, Tan G, Yang D, Chou CJ, Sole J, Nichols A, Ross JS, Tartaglia LA, and Chen H (2003). Chronic inflammation in fat plays a crucial role in the development of obesity-related insulin resistance. J. Clin. Invest 112, 1821–1830. [PubMed: 14679177]

Yeop Han C, Kargi AY, Omer M, Chan CK, Wabitsch M, O'Brien KD, Wight TN, and Chait A (2010). Differential effect of saturated and unsatu-rated free fatty acids on the generation of monocyte adhesion and chemotactic factors by adipocytes: dissociation of adipocyte hypertrophy from inflammation. Diabetes 59, 386–396. [PubMed: 19934003]

Yu S, Dong J, Zhou W, Yang R, Li H, Zhao H, Zhang T, Guo H, Wang S, Zhang C, and Chen W (2014). A rapid and precise method for quantification of fatty acids in human serum cholesteryl esters by liquid chromatography and tandem mass spectrometry. J. Chromatogr. B Analyt. Technol. Biomed. Life Sci 960, 222–229.

Zhang F, Zheng L, Cheng S, Peng Y, Fu L, Zhang X, and Linhardt RJ (2019). Comparison of the Interactions of Different Growth Factors and Glycosaminoglycans. Molecules 24, 3360.

Zizola CF, Julianelli V, Bertolesi G, Yanagishita M, and Calvo JC (2007). Role of versican and hyaluronan in the differentiation of 3T3-L1 cells into preadipocytes and mature adipocytes. Matrix Biol 26, 419–430. [PubMed: 17513099]

Highlights

- Versican derives from adipocytes in obese adipose tissue
- Adipose tissue macrophages are the major source of biglycan in obesity
- Adipocyte-specific ablation of versican attenuates inflammation and insulin resistance
- Macrophage-specific deficiency of biglycan improves adipose tissue inflammation

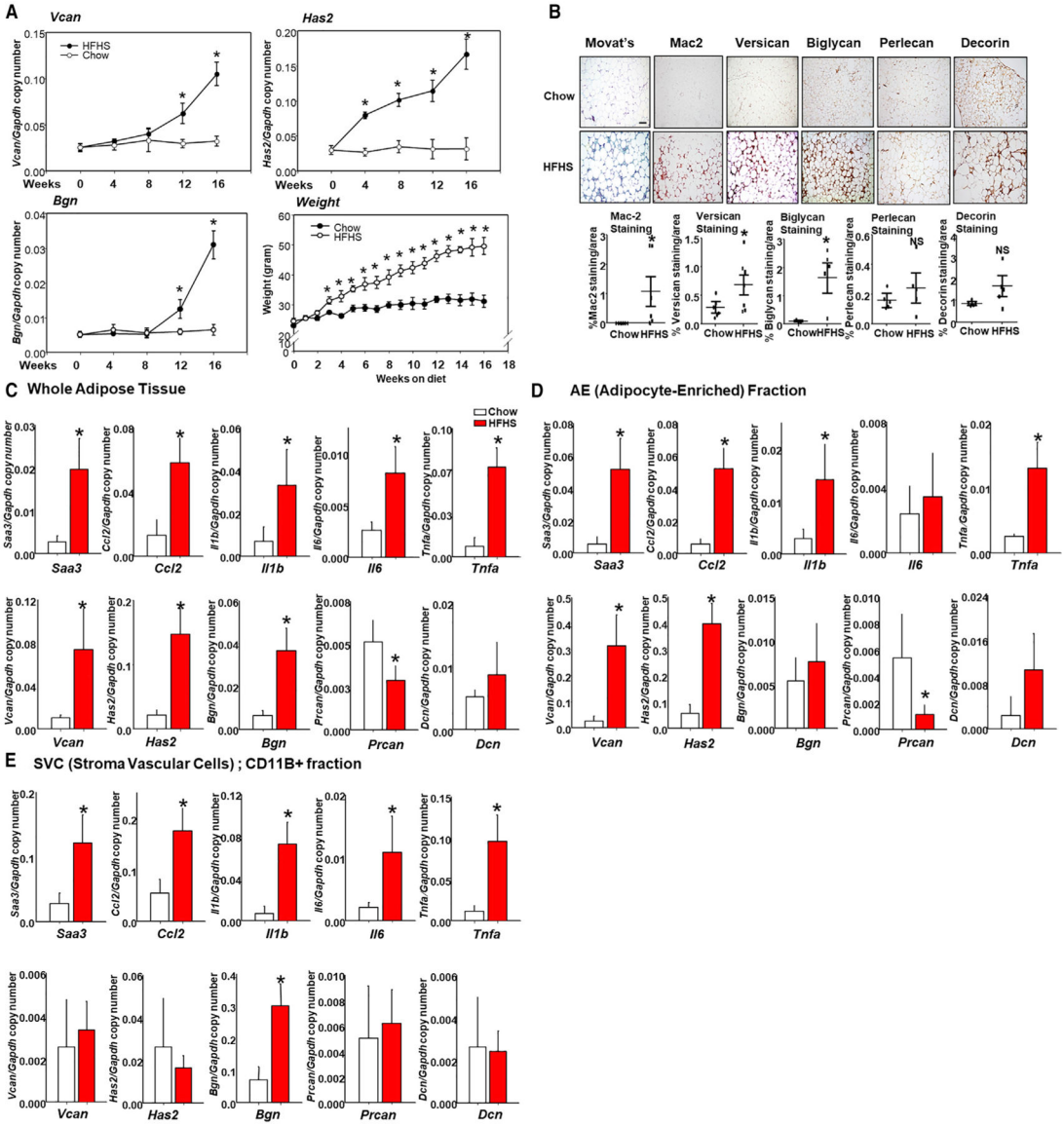

Figure 1. Versican Is Increased in the Adipocyte-Enriched (AE) Fraction of Adipose Tissue, whereas Biglycan Is Mainly Increased in the Macrophage-Enriched (CD11B+) Fraction in Epididymal Adipose Tissue from Mice Fed a High-Fat, High-Sucrose (HFHS) Diet

(A) Epididymal fat isolated from wild-type mice fed a HFHS diet or chow for 4, 8,12, and 16 weeks was analyzed by RT-PCR using *Vcan*, *Has2*, and *Bgn* probes (n = 5, mean ± standard error of the mean [SEM]).

(B) Mice were fed a chow or HFHS diet for 16 weeks, and then adipose tissue was obtained and immunostained with the antibodies shown (top panel). Tissues were photographed using microscopy (original magnification, ×60; scale bar, 100 μm). Quantification of the immunostaining is shown in the bottom panel (n = 5–7, mean ± SEM). *p < 0.001 versus chow.

(C–E) Epididymal fat pads from wild-type (WT) mice fed a chow or HFHS diet for 16 weeks were collagenase digested to separate the AE and macrophage-enriched fractions with a CD11B antibody. AE and macrophage-enriched fractions were confirmed by *Adipoq* and

Cd68 gene expression, respectively. (C) Whole adipose tissue; (D) AE fraction; and (E) macrophage-enriched fraction. Gene expression for chemokines, cytokines, and proteoglycans was determined by RT-PCR (n = 5, mean ± SEM). *$p < 0.05$ versus chow. ANOVA and Bonferroni post hoc test.

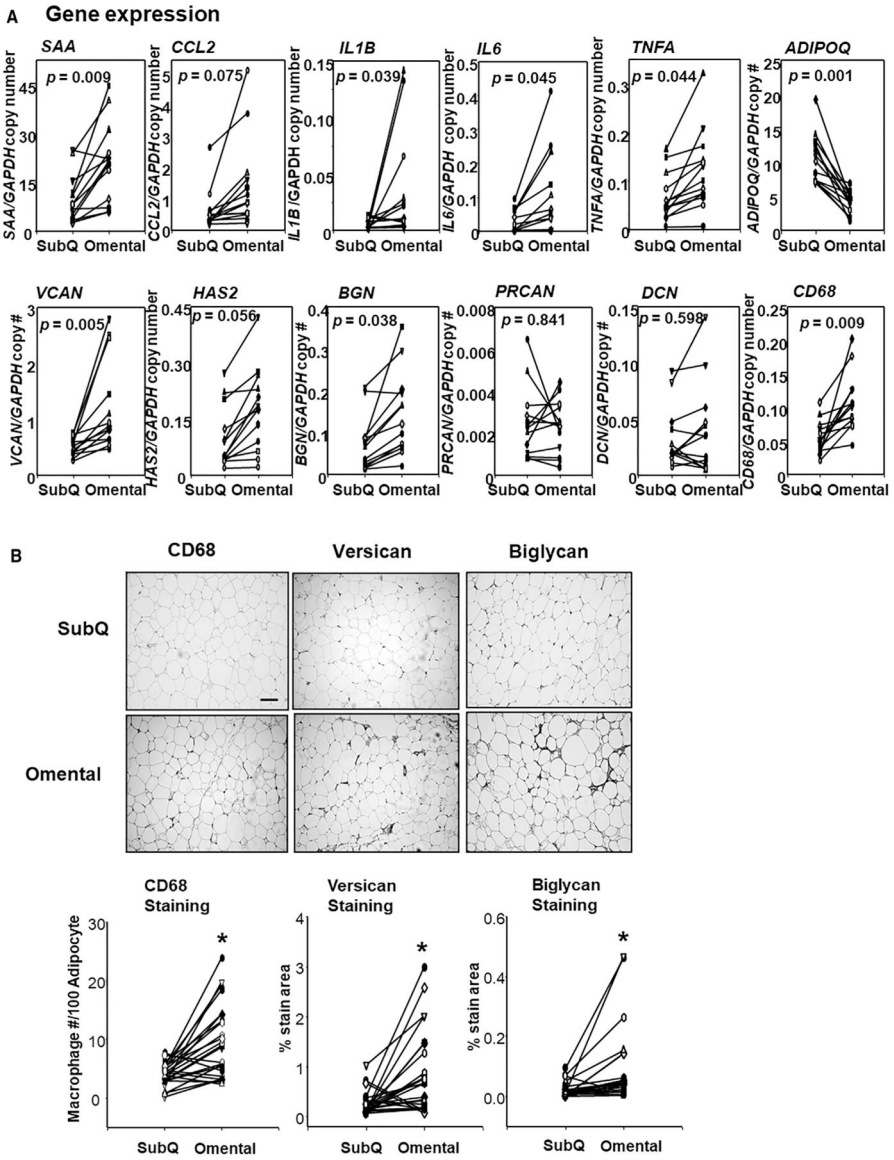

Figure 2. Versican and Biglycan Are Increased in Omental Fat Compared with Subcutaneous Fat Tissue from Obese Human Subjects Undergoing Gastric Bypass Surgery

(A) Chemokine, cytokine, and proteoglycan gene expression in subcutaneous (s.c.) and omental fat pads from subjects undergoing gastric bypass surgery was analyzed by RT-PCR (n = 13, mean ± SEM). *p < 0.05 versus s.c., Student's t test.

(B) s.c. and omental fat obtained from subjects undergoing gastric bypass surgery were immunostained with the antibodies shown (n = 24, top panel). Tissues were photographed using microscopy (original magnification, 360; scale bar, 100 mm). Quantification of the immunostaining is shown in the bottom panel (n = 24, mean ± SEM). *p < 0.001 versus s.c., Student's t test.

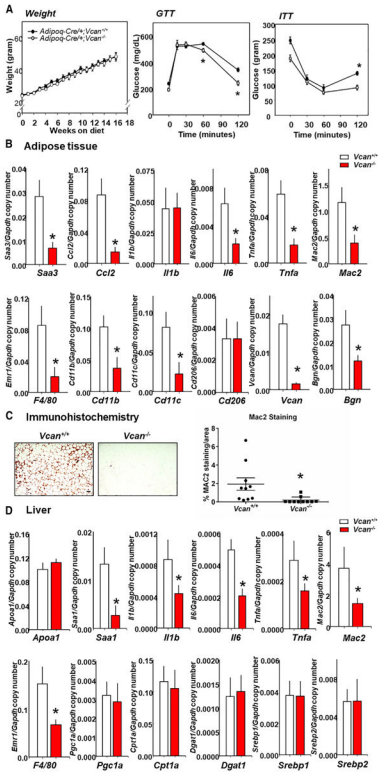

Figure 3. Adipocyte-Specific Deficiency of Versican Improves Adipose Tissue Inflammation, Liver Inflammation, Glucose Tolerance, and Insulin Sensitivity after 16 Weeks on a HFHS Diet

(A) *Adipoq-Cre/+;Vcan*$^{+/+}$ and *Adipoq-Cre/+;Vcan*$^{Flox/Flox}$ mice were fed a HFHS diet for 16 weeks (n = 10, mean ± SEM). Body weights, glucose tolerance, and insulin tolerance were measured at the indicated time points. *p < 0.01 versus *Adipoq-Cre/+;Vcan*$^{+/+}$.

(B) *Saa3*, *Ccl2*, *Il1*b, *Il6*, *Tnfa*, *Mac2*, *F4/80*, *Cd11b*, *Cd11c*, *Cd206*, *Vcan*, and *Bgn* gene expression was measured in epididymal fat by RT-PCR.

(C) Epididymal fat was analyzed by immunohistochemistry using a Mac2 antibody, which detects macrophages (n = 10, mean ± SEM). Tissues were photographed using microscopy (original magnification, 360; scale bar, 100 mm) and quantified using Image Pro Plus software. *p < 0.05 versus *Adipoq-Cre/+;Vcan*$^{+/+}$ in HFHS.

(D) *Apoa1*, *Saa1*, *Tnfa*, *Il1b*, *Il6*, *Mac2*, *F4/80*, *Pgc1α*, *Cpt1α*, *Dgat1*, *Srebp1*, and *Srebp2* gene expression was measured in the liver by RT-PCR (n = 10, mean ± SEM). ANOVA and Bonferroni post hoc test.

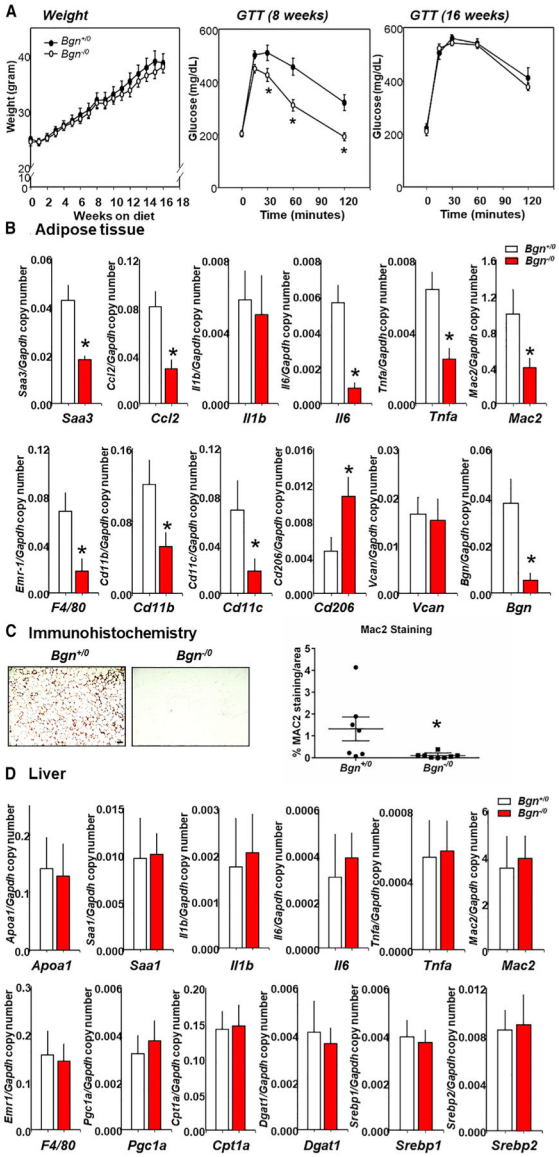

Figure 4. Bone Marrow-Specific Chimeric Biglycan Deficiency Delays Onset of Glucose Intolerance and Improves Adipose Tissue Inflammation

Male CD45.1 isotype C57BL/6 mice were transplanted with bone marrow cells from CD45.2 isotype WT (n = 7) or CD45.2 isotype $Bgn^{-/0}$ mice (n = 8). After a 2-week recovery period, mice were fed a HFHS diet for 16 weeks.

(A) Body weights and glucose tolerance were measured at the indicated time points (mean ± SEM). *p < 0.01 versus $Bgn^{+/0}$.

(B) *Saa3*, *Ccl2*, *Il1β*, *Il6*, *Tnfa*, *Mac2*, *F4/80*, *Cd11b*, *Cd11c*, *Cd206*, *Vcan*, and *Bgn* gene expression was measured in epididymal fat after 16 weeks on the HFHS diet by RT-PCR (mean ± SEM).

(C) Epididymal fat after 16 weeks on the HFHS diet was analyzed by immunohistochemistry using a Mac2 antibody, which detects macrophages (n = 7–8, mean ± SEM). Tissues were photographed using microscopy (original magnification, 360; scale bar, 100 μm) and quantified using Image Pro Plus software. *p < 0.05 versus $Bgn^{+/0}$ in HFHS.

(D) *Apoa1*, *Saa1*, *Tnfa*, *Ilb*, *Il6*, *Mac2*, *F4/80*, *Pgc1a*, *Cpt1a*, *Dgat1*, *Srebp1*, and *Srebp2* gene expression was measured in the liver after 16 weeks on the HFHS diet by RT-PCR (n = 7– 8, mean ± SEM). ANOVA and Bonferroni post hoc test.

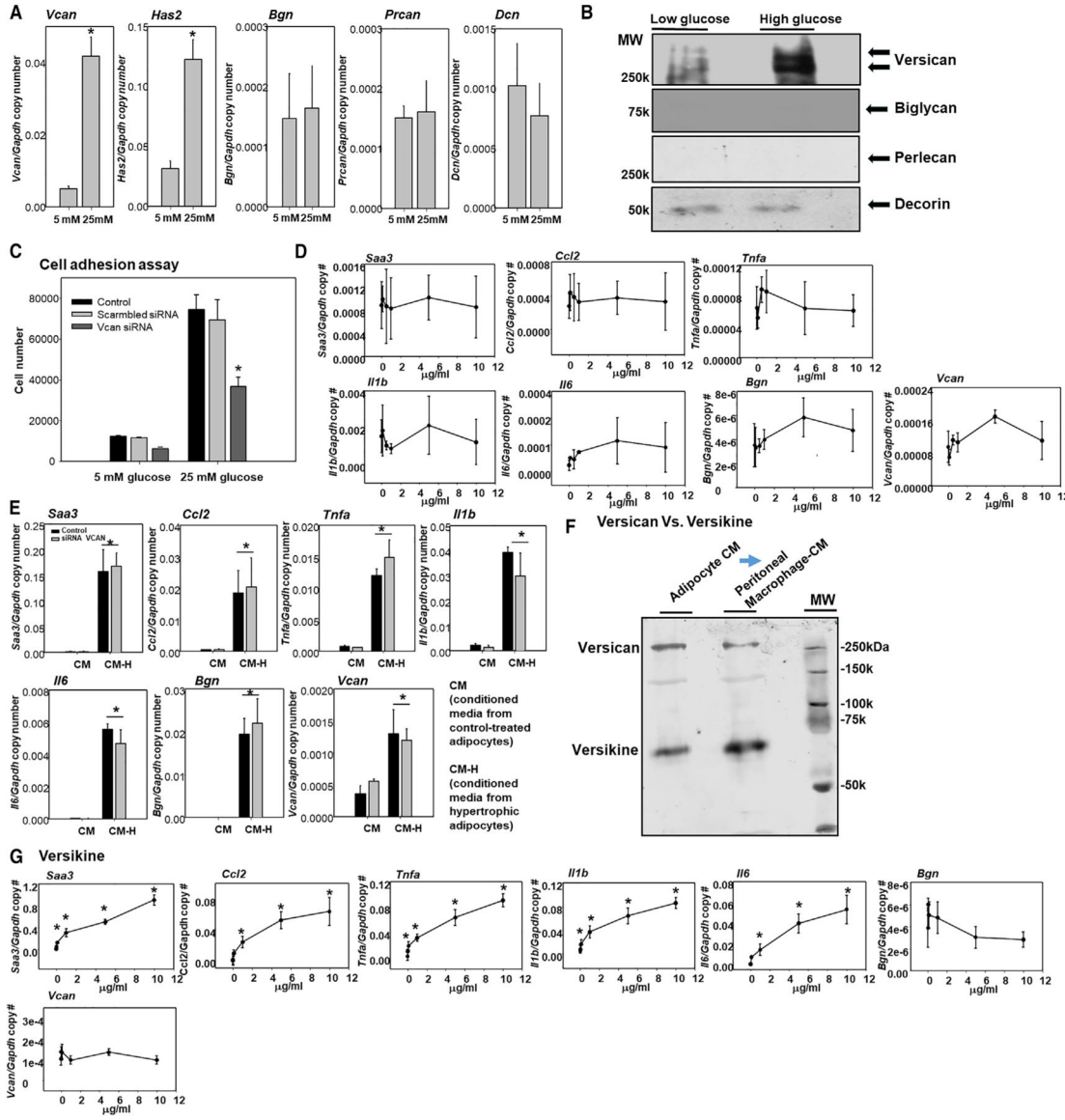

Figure 5. Versican Increases in 3T3-L1 Adipocytes Made Hypertrophic by Exposure to High-Glucose Conditions, and Versikine, which Is Derived from Versican, Increases Macrophage Inflammation

Differentiated 3T3-L1 adipocytes were cultured for 7 days in low-glucose (5 mmol/L) or high-glucose (25 mmol/L) medium.

(A and B) After 7 days of treatment, proteoglycan gene expression was analyzed by RT-PCR (A) and cell supernatants were analyzed by immunoblotting using versican, biglycan, perlecan, and decorin-specific antibodies (B). Data are representative of 4 independent experiments with mean ± SEM. *$p < 0.001$ versus 5 mM glucose. Student's t test.

(C) Monocyte adhesion to 3T3-L1 hypertrophic adipocytes that were or were not been pre-treated with *Vcan* siRNA was measured using calcein-AM-labeled U937 monocytes as described in STAR Methods. Data are representative of 3 independent experiments with mean ± SEM. *$p < 0.001$ versus 25 mM glucose control. ANOVA and Bonferroni post hoc test.

(D and E) Purified versican (D) or conditioned medium from untreated or hypertrophic adipocytes (CM or CM-H, respectively) with or without silencing versican (E) was added to quiescent RPMs for 24 h. Data are representative of 3 independent experiments with mean ± SEM. *$p < 0.001$ versus CM. ANOVA and Bonferroni post hoc test.

(F) Versican and versikine were analyzed by western blot using a versikine antibody in adipocyte-conditioned medium and in the medium from RPM that had been incubated with adipocyte-conditioned medium.

(G) Purified versikine was added to RPMs for 24 h. Data are representative of 6 independent experiments with mean ± SEM. *$p < 0.001$ versus the non-treated control. ANOVA and Bonferroni post hoc test.

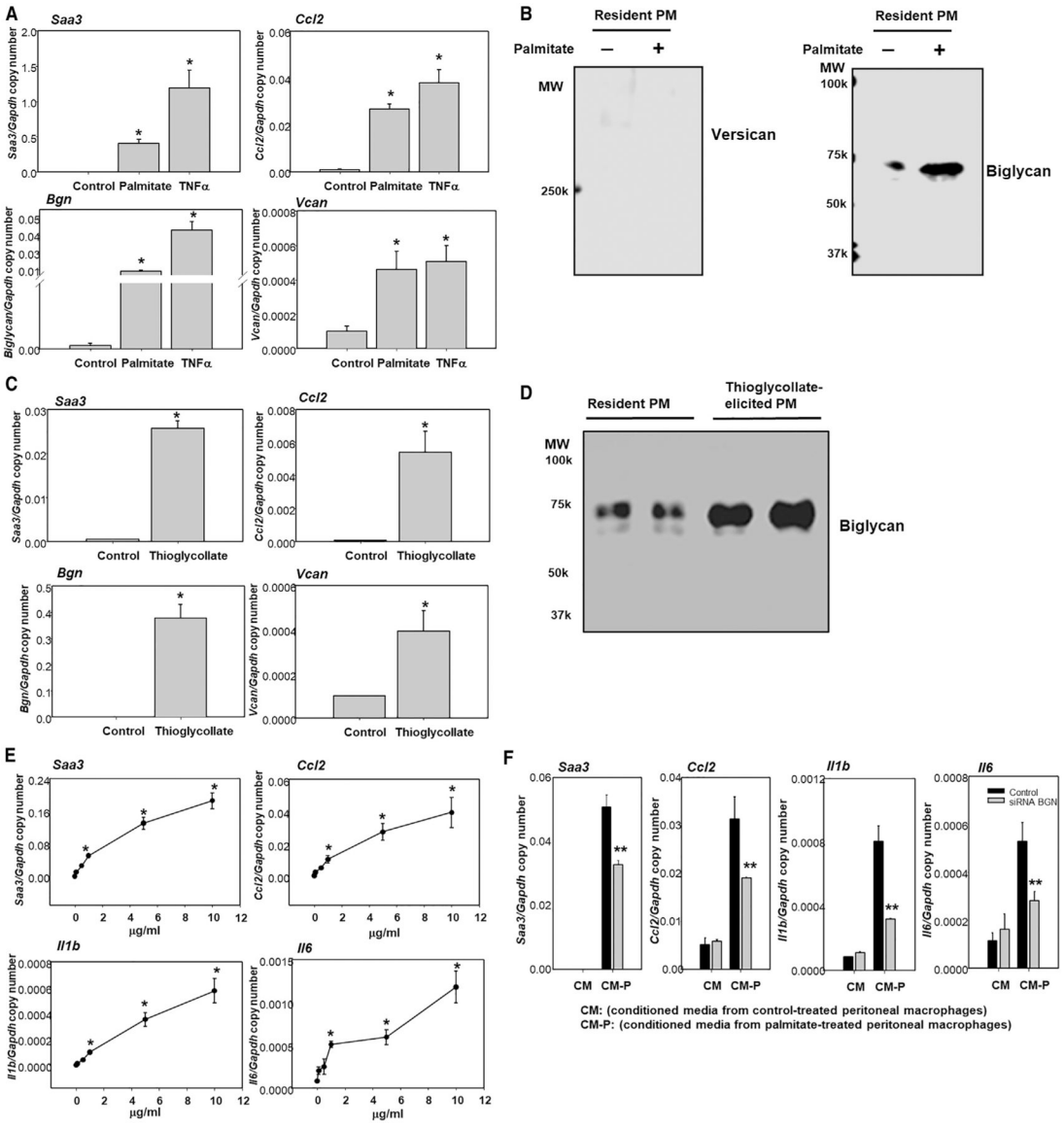

Figure 6. Macrophage-Derived Biglycan from Palmitate-Induced RPMs and Thioglycollate-Elicited Peritoneal Macrophages Induces Adipocyte Inflammation

(A–D) Resident peritoneal macrophages (RPMs) (A and B) were incubated with palmitate (50 μmol/L) or TNF-α (10 ng/mL) for 24 h, or thioglycollate-elicited peritoneal macrophages were isolated (C and D). *Saa3*, *Ccl2*, *Bgn*, and *Vcan* gene expression (A and C) were measured by RT-PCR, and cell supernatants (B and D) were analyzed by immunoblotting using versican and biglycan antibodies. Data are representative of 5 independent experiments with mean ± SEM. *$p < 0.001$ versus control. ANOVA and Bonferroni post hoc test.

(E and F) Purified biglycan (E) or conditioned medium from RPMs with or without silencing biglycan (F) was added to 3T3-L1 adipocytes for 24 h. Chemokine and cytokine gene expression was measured by RT-PCR. Data are representative of 3 independent

experiments with mean ± SEM. *p < 0.001 versus control, **p <0.001 versus CM-P without siRNA. ANOVA and Bonferroni post hoc test.

Table 1.

Plasma Variables on the HFHS Diet (Control versus Adipoq-Cre/+;Vcan$^{Flox/Flox}$ Mice)

Genotype	Insulin (ng/mL)	Adiponectin (μg/mL)	SAA (μg/mL)	Triglycerides (mg/dL)	Cholesterol (mg/dL)	NEFA (mmol/L)
Control	5.30 ± 0.60	29.04 ± 2.13	68.15 ± 21.92	51.17 ± 3.02	177.02 ± 13.21	0.86 ± 0.04
Vcan$^{-/-}$	3.55 ± 0.44 *	45.68 ± 3.20 *	22.29 ± 2.01 *	59.46 ± 3.41	181.96 ± 6.68	0.92 ± 0.05

Values represent mean ± SEM (n = 10–12 per group).

* $p < 0.05$ versus control mice on the HFHS diet.

KEY RESOURCES TABLE

REAGENT or RESOURCE	SOURCE	IDENTIFIER
Antibodies		
CD2368	Agilent	#M087601–2, RRID:AB_2074844
Mac2	R&D	# AF1197, RRID:AB_2234687
Versican	Millipore	# AB1033, RRID:AB_90462
Biglycan	Thermo Fisher Scientific	#PA5–76821, RRID:AB_2720548
Perlecan	Thermo Fisher Scientific	#MA1–06821, RRID:AB_559394
Decorin	Thermo Fisher Scientific	#PA5–95830, RRID:AB_2807632
Versikine	Thermo Fisher Scientific	# PA1-1748A, RRID:AB_2304324
PE CD45.1	eBioscience	#12-0453-82, RRID:AB_465675
APC CD45.2	Biolegend	#109814, RRID:AB_389211
BV 605 CD3e	Biolegend	#100351, RRID:AB_2565842
Percp Cy5.5 Ly6G/Gr	eBioscience	#45–5931-80, RRID:AB_906247
FITC CD11b	eBioscience	#11–0112-82, RRID:AB_464935
BV 650 CD19	Biolegend	#115541, RRID:AB_11204087
eFluor 450 F4/80	eBioscience	#48–4801-82, RRID:AB_1548747
NFkB p65	Cell Signaling	#8242, RRID: AB_10859369
NFkB p65 ser 536	Cell Signaling	#3033, RRID: AB_331284
Akt	Cell Signaling	#9272, RRID: AB_329827
Akt ser 473	Cell Signaling	#4060, RRID: AB_2315049
Chemicals, Peptides, and Recombinant Proteins		
Versikine	This paper	N/A
HFHS diet	BioServ	# F4997
Collagenase	Worthington	#M2D5542
Glucose	Sigma	#G7021
Insulin	Lilly	#HI-210
DMEM (low glucose)	Hyclone	#SH30021.01
DMEM (high glucose)	Hyclone	#SH30243.01
RPMI 1640	Hyclone	#SH30027.01
Phenol red-free RPMI 1640	GIBCO	#11835030
FBS	Hyclone	#SH30396.03
EX-CELL 293	Sigma	#14571c
IFN-g	R&D	#485-MI
LPS	Cayman Chemical	#19660
IL4	R&D	#404-ML
Thioglycollate	BD	#221195
Palmitate	Sigma	#P-0500
NaOH	Sigma	#S3183
Albumin	Sigma	#A8806
Chondroitin ABC lyase	Sigma	# C-3667
DEAE Sephacel	Sigma	#I-6505

REAGENT or RESOURCE	SOURCE	IDENTIFIER
Aqua Block	EastCost Bio	#PP-82
Strep Tactin column	IBA	#2–1505-101
NIR Zombie	Biolegend	#423105
Fc Block	BD	#553142
Dexamethasone	Sigma	#D4902
3-isobutyl-1-methylxanthine	Sigma	#I7018
Bovine insulin	Sigma	#10516
Indomethacin	Sigma	#I7378
Rosiglitazone	Cayman Chemical	#71740
Calcein-AM	Molecular Probes	#C3100MP
HCS LipidTOX	Invitrogen	#H34475
ACK RBC lysis buffer	Thermo Fisher Scientific	#A1049201
Biglycan	R&D	#8128-CM
TaqMan Master kit	Thermo Fisher Scientific	#4324018
Paraformaldehyde	Sigma	#6148
Optima LC-grade water	Fisher	#W6500
Ammonium bicarbonate	Sigma	#09830
Trizma base	Sigma	#93362
Neutral-buffered formalin	Fisher	#245–685
Urea	Sigma	#U5378
Critical Commercial Assays		
anti-CD11b immunoaffinity isolation kit	Miltenyi Biotec	#18970A
Insulin ELISA kit	Millipore	#EZRMI13K
Adiponectin ELISA kit	Millipore	#EZMADP60K
SAA ELISA kit	R&D	#DY294805
NEFA Assay kit	Wako	#993–35191
Cholesterol Assay kit	Stanbio	#1010225
Triglyceride Assay kit	Stanbio	#2100225
DeliverX system	Panomics	#DX0004
Experimental Models: Cell Lines		
3T3-L1	ATCC	#CRL-3242, RRID:CVCL_0A20
Human SGBS	Lin et al., 2005	N/A
HEK293/17	ATCC	# ACS4500, RRID:CVCL_4V93
U937	ATCC	#CRL-1593.2, RRID:CVCL_0007
Experimental Models: Organisms/Strains		
Mouse: WT C57BL/6J	Jackson Laboratory	#000664, RRID:IMSR_JAX:000664)
Mouse: Adipoq-Cre	Dr. Philip Scherer	N/A
Mouse: Adipoq-Cre/+;Vcan$^{Flox/Flox}$	This paper	N/A
Mouse: *Adipoq-Cre/+;Vcan$^{+/+}$*	This paper	N/A
Mouse: *BGN-$^{/0}$*	Dr. David Birk	N/A
Mouse: C57BL/6 (CD45.1)	Charles River	#564, RRID:IMSR_CRL:564
Mouse: transplanted *Bgn$^{+/0}$*	This paper	N/A

REAGENT or RESOURCE	SOURCE	IDENTIFIER
Mouse: transplanted *Bgn*$^{-/0}$	This paper	N/A
Oligonucleotides		
siRNA for versican	Ambion	#MSS273870
siRNA for biglycan	Ambion	#AM16708
Primers for RT-PCR	See Table S1	N/A
Primers for genotyping	See STAR Methods	N/A
Software and Algorithms		
SPSS v.19	IBM	https://www.ibm.com/products/spss-statistics
OriginPro v.8.6	Origin Laboratory	https://www.originlab.com/origin
Dexamethasone	Sigma	#D4902
3-isobutyl-1-methylxanthine	Sigma	#I7018
Bovine insulin	Sigma	#10516
Indomethacin	Sigma	#I7378
Rosiglitazone	Cayman Chemical	#71740
Calcein-AM	Molecular Probes	#C3100MP
HCS LipidTOX	Invitrogen	#H34475
ACK RBC lysis buffer	Thermo Fisher Scientific	#A1049201
Biglycan	R&D	#8128-CM
TaqMan Master kit	Thermo Fisher Scientific	#4324018
Paraformaldehyde	Sigma	#6148
Optima LC-grade water	Fisher	#W6500
Ammonium bicarbonate	Sigma	#09830
Trizma base	Sigma	#93362
Neutral-buffered formalin	Fisher	#245–685
Urea	Sigma	#U5378
Critical Commercial Assays		
anti-CD11b immunoaffinity isolation kit	Miltenyi Biotec	#18970A
Insulin ELISA kit	Millipore	#EZRMI13K
Adiponectin ELISA kit	Millipore	#EZMADP60K
SAA ELISA kit	R&D	#DY294805
NEFA Assay kit	Wako	#993–35191
Cholesterol Assay kit	Stanbio	#1010225
Triglyceride Assay kit	Stanbio	#2100225
DeliverX system	Panomics	#DX0004
Experimental Models: Cell Lines		
3T3-L1	ATCC	#CRL-3242, RRID:CVCL_0A20
Human SGBS	Lin et al., 2005	N/A
HEK293/17	ATCC	# ACS4500, RRID:CVCL_4V93
U937	ATCC	#CRL-1593.2, RRID:CVCL_0007
Experimental Models: Organisms/Strains		
Mouse: WT C57BL/6J	Jackson Laboratory	#000664, RRID:IMSR_JAX:000664)
Mouse: Adipoq-Cre	Dr. Philip Scherer	N/A

REAGENT or RESOURCE	SOURCE	IDENTIFIER
Mouse: Adipoq-Cre/+;Vcan$^{Flox/Flox}$	This paper	N/A
Mouse: *Adipoq-Cre/+;Vcan$^{+/+}$*	This paper	N/A
Mouse: *BGN$^{-/0}$*	Dr. David Birk	N/A
Mouse: C57BL/6 (CD45.1)	Charles River	#564, RRID:IMSR_CRL:564
Mouse: transplanted *Bgn$^{+/0}$*	This paper	N/A
Mouse: transplanted *Bgn$^{-/0}$*	This paper	N/A
Oligonucleotides		
siRNA for versican	Ambion	#MSS273870
siRNA for biglycan	Ambion	#AM16708
Primers for RT-PCR	See Table S1	N/A
Primers for genotyping	See STAR Methods	N/A
Software and Algorithms		
SPSS v.19	IBM	https://www.ibm.com/products/spss-statistics
OriginPro v.8.6	Origin Laboratory	https://www.originlab.com/origin
Prism v. 6.0	GraphPad	https://www.graphpad.com/scientific-software/prism/
Image Pro v.6.0	Media Cybernetics	https://www.mediacy.com/imageproplus
FlowJo v.10	Treestar	https://www.flowjo.com
Excel (365 Pro)	Microsoft	https://www.microsoft.com/en-us/microsoft-365/excel
Other		
FusionTM Series Universal Microplate Analyzer	Packard Bioscience	N/A
LI-COR Odyssey® scanner	LI-COR Biotechnology	N/A
ABI prism 7900HT system	Applied Biosystems	N/A
LSRII flow cytometer	BD	N/A